AN APPLICATION OF REGULARIZED SPECTRAL ENTROPY FOR DETECTION OF TASK-RELATED INFORMATION CONTENT IN FMRI

by

Christopher Barry Proctor O'Grady

Submitted in partial fulfilment of the requirements
for the degree of Master of Science

at

Dalhousie University
Halifax, Nova Scotia
August 2017

To my dear friend Elisabeth,
who has always been the best example of kindness,
humility, and integrity. And to my mother,
who is the smartest brain I ever scanned.

Table of Contents

List of Figures

Abstract

Functional MRI (fMRI) has become a critical tool for clinical evaluation and neuroimaging research in recent years. This work investigates a unique application of spectral entropy (Shannon's entropy in the frequency domain) combined with a regularization scheme for an ill-fitted problem to identify the presence of useful task-related information content in fMRI scans. Regularized spectral entropy was compared to traditional methods of identifying useful information such as the General Linear Model (GLM), as well as known percent signal change in simulated data sets created with noise parameters informed by real data sets, and signal-to-noise ratio (SNR) in idealized signals. Combined with regularization, spectral entropy was found to have comparable sensitivity and specificity to the GLM, as well as a correlated response to percent signal change and SNR. Additionally, spectral entropy was fast to compute and required minimal a priori information compared to other methods used to identify useful task-related information.

List of Abbreviations

BOLD: blood oxygen level dependent

CBV: cerebral blood volume

EEG: electroencephalography

EPI: echo-planar imaging

eSAM: etomidate speech and memory

fMRI: functional MRI

fMRIB: functional MRI of the brain

FN: false negative

FP: false positive

FSL: functional MRI of the brain software library

GLM: general linear model

HCP: human connectome project

ICA: independent components analysis

NVC: neurovascular coupling

RF: radiofrequency

ROC: receiver-operator characteristic

ROI: region of interest

TE: echo time

TN: true negative

TNR: true negative rate

TP: true positive

TPR: true positive rate

TR: repetition time

Acknowledgements

I would like to sincerely thank my supervisor, Dr. Steven Beyea, for welcoming me in his lab as a graduate student and guiding my work. Also, my co-supervisor, Dr. Javeria Hashmi, and committee members, Dr. Antonina Omisade and Dr. James Rioux for their invaluable help. I truly appreciate the amount of knowledge and passion all four of you have shared with me.

I would also like to thank Carl Helmick, the MRI technologists in the Halifax Infirmary, Dr. James Robar and the faculty and students in Medical Physics at Dalhousie University, and the staff at BIOTIC. I am especially grateful for the help of Dr. Steve Patterson, for his work on the simulated data I used in this research, and his very helpful input throughout.

The following people have provided particularly incredible support and friendship throughout my degree and before, and I would like to express my gratitude to all of them: Eileen, Elisabeth, Eva G., Eva S., Hoi Bing, James, John, Jonathan, Katie, Linda, Lissy, Loree, Manjari, Melissa, Nina, Neville, Dr. Richard Lee, Tareq, Tonya, and of course – my mother.

Chapter 1: Introduction

This work is a novel application of information theory to functional MRI (fMRI), motivated by the goal of detecting useful task information in raw signals. The reasoning behind use of raw or minimally processed signals is to rapidly detect task-relevant information immediately after the scan, or ideally during the scan itself. Detecting the presence of useful information quickly is critical in an fMRI scan because of the considerably greater time involved in post-processing and analysis; it may take hours or even days to fully process the data, and if the patient has left, it may not be possible to re-scan the patient should the data quality be low. In this work, spectral entropy is used for the first time in fMRI analysis and works in concert with a data-driven regularization scheme to quickly elucidate if data will contain useful task-related information.

1.1 Introduction to fMRI

fMRI was originally introduced in 1992 by Peter Bandettini (Bandettini, Wong, Hinks, Tikofsky, and Hyde, 1992), after the discovery of the Blood Oxygen Level Dependent signal contrast by Seiji Ogawa et al. just a few years earlier (Ogawa, Lee, Nayak, and Glynn, 1990; Ogawa, Lee, Kay, and Tank, 1990). The basis of fMRI is neurovascular coupling (NVC). When neurons are stimulated and respond by firing action potentials, they consume energy and oxygen while producing metabolic byproducts. In response, blood vessels surrounding brain tissue that is being used increases in cerebral blood volume (CBV) by approximately 10% (Buxton, 2013). This is an overcompensation compared to the actual metabolic demand and results in a higher concentration

of oxygenated blood in active brain regions. This change can then be detected using Blood Oxygen Level Dependent (BOLD) contrast imaging.

1.2 Clinical Applications of fMRI

Originally used primarily for research, the range of applications of fMRI has grown exponentially and it is now a clinically used tool for presurgical planning and determining language laterality (Jansen et al., 2006; Stippich, 2010). This has created a demand for development of better processing and analysis methods, as well as related procedures ensuring that the scan quality is suitably high for clinical application. These are often related to inherent challenges in fMRI, such as guaranteeing patient compliance or minimizing noise sources. Patient compliance is critical as the individual must be accurately performing the task and contrast to activate the desired brain regions. If patients misunderstand task instructions, lose focus, or do not complete the tasks for various other reasons, the scan quality will be compromised.

The benefits of fMRI strongly outweigh the challenges, however. Greatest among these is the better spatial resolution relative to cheaper methods such as electroencephalography (EEG). Another key benefits of fMRI in the clinic is that it is non-invasive and relatively fast for the patient. Many tests, such as for determining language laterality, take multiple days or at least half-days. Additionally in the case of determining language laterality, fMRI has good agreement with other methodologies as well as some notable unique benefits. One study found up to 90% agreement between fMRI and the Wada test (currently the gold standard for determining language laterality) in a cohort of 229 patients with epilepsy (Janecek et al., 2013). The Wada test is a two-day

invasive procedure involving sedation of one brain hemisphere via an injection through the internal carotid arteries after insertion of a catheter in the femoral artery (Wada, 1949). The Etomidate Speech and Memory (eSAM) test is an improvement on the Wada test, but is still a two day procedure and uses the same principles of an invasive catheter injection (Jones-Gotman, Sziklas, and Djordievic, 2009). Language lateralization using fMRI typically only requires half an hour for a patient and is completely non-invasive, making it a desirable alternative.

Other clinical applications of fMRI include identification of the motor cortex for presurgical patients, as well as more novel applications predicting surgical outcomes (Negishi, Martuzzi, Novotny, Spencer, and Constable, 2011). While the number of novel potential clinical applications increases, the core clinical use of fMRI remains identification of functional regions and hemispheric language localization.

1.3 fMRI Analysis

The analysis method of fMRI data is critical to the outcome and how the results are interpreted. The most common analysis method began in 1994 when Karl Friston introduced the General Linear Model (GLM), which is a sophisticated parametric model for the analysis of fMRI signals (Friston et al., 1994). The GLM relies on an assumed haemodynamic response function – an expected way in which cerebral

Figure 1.1 An example of an fMRI language map. Areas in bright yellow correspond to high t-statistic values and represent areas of activation.

blood volume fluctuates with regards to activation. Through convolution of the haemodynamic response to the task on/off diagram, the "perfect" fMRI signal is found (the signal that would come from a voxel perfectly responding to the task). Statistical comparison of this signal to actual signals produces a map of activation that can be roughly described as a map of the statistical likelihood that any given voxel is responding to the task. In the interest of saving detail for later chapters, if a low t-statistic value is calculated for a voxel using a t-test, it's considered unlikely that the signal from that voxel is due to the task. Conversely, a high t-statistic value suggests that it is highly likely the signal in a voxel is due to a task. An example of such an fMRI map is given in figure 1.1.

To accurately compute statistics like the t-statistic with the GLM, effective pre-processing is necessary. Pre-processing is also important to briefly address with regards to fMRI analysis, not only because it has always been a contentious topic, but because of its role in influencing fMRI results, and relationship to sources of noise. Pre-processing is a broad term in fMRI analysis that refers to steps taken prior to statistical analysis to counteract sources of noise or other confounding factors in the data, or to improve statistical power in the calculations. These include but are not limited to: realigning frames to counteract the effect of motion, slice-timing correction to adjust for intensity differences due to the order in which slices were collected within the MRI, spatial smoothing with a Gaussian kernel to increase signal-to-noise ratio (SNR) and make the error distributions more normal for statistical testing, and either rigid-body or affine transformation to fit the functional data to the anatomical anatomy (or to standard data, such as the MNI brain) (Smith, 2004). Affine transformations are used to counteract distortion of anatomy that is common in echo-planar imaging

(EPI) used for fMRI, but may be replaced by a simple rigid-body transformation depending on scan parameters. Additionally, skull-stripping and removal of other non-brain voxels is performed to avoid calculation on voxels that are known to definitely not be responding to the task. These processing steps are relatively time consuming and cannot be performed "online", and must therefore be done after the data is transferred off the MRI and make interpreting a statistical map not an effective means of fast scan quality determination.

1.4 Challenges of fMRI and Data Quality Correction Methods

As mentioned previously with regards to language laterality, fMRI does not enjoy complete agreement with gold standard methods. The reasons for this may be due to lack of standardized fMRI paradigms and resulting inconsistent results (Desmond and Chen, 2002), or to technical or acquisition issues. The fMRI paradigm is obviously critical to fMRI quality, but is not the focus of the discussion here and it is assumed that the paradigm is well-designed and the key factors influencing data quality are technical, or acquisition-related such as if the patient is actually completing the task as intended. Some of the main challenges in ensuring high quality fMRI data are discussed below.

1.4.1 Motion

Motion is probably the most discussed source of noise and poor data quality in fMRI, and numerous correction methods have been devised. The most basic is rigid-body realignment, where each 3D image from every acquisition or repetition time (TR) is realigned to the first frame or the anatomical image. More sophisticated methods are primarily used for resting state analysis, which is more sensitive to motion (Satterthwaite et al., 2013). These include regression of

motion parameters from the signal, wavelet filtering, and scrubbing or interpolating. Regression may be used for task-based scans in extreme cases of motion, and simply involves calculation of motor parameters and their subsequent removal from signal (Power, Schlagger, and Peterson, 2015). Scrubbing simply removes time points that coincide with motion parameters exceeding a set threshold (and often removal of the previous and following time points as well), and interpolation is when these data points are replaced by an interpolated value (typically taken from a mean of the two data points surrounding those removed) (Power, Schlagger, and Peterson, 2015). Scrubbing is a very common method of removing motion affected data in task-based fMRI, provided that not too substantial a number of data points are removed. It is typically performed after rigid body alignment to remove signal spikes created by motion.

The challenge with motion is that no correction is perfect, and as one author recently highlighted, *motion correction is a goal, not a method* (Yakupov, Lei, Hoffman, and Speck, 2017). The amount of motion interference with the desired information is what is important, not the motion itself. Motion may result in minimal distortion of the desired signal and therefore only marginally affect its quality, or it may add significant noise to the signal but still result in the same clinical decision. Determining and quantifying the quality of data with regards to motion must take into account not only how much motion has occurred, but how the data is impacted. Moreover, motion correction methods may introduce new artifacts and these must be carefully considered as well.

1.4.2 Task Adherence and Response

Assuming that the fMRI task is well-designed and correctly administered, there are few ways to ensure that the subject or patient is actually compliant and completing the task. Video monitoring is one option, but many fMRI tasks are covert and not observable via video or microphone. Language scans, for instance, are typically degraded by the motion associated with overt responses, and motor activation due to speech is undesired. Post-scan interviews can help ensure some adherence by soliciting participant feedback, but cannot prove that the patient fully understood the instructions within the scanner.

Some modern MRI scanners have real-time maps that can be viewed during the scan. These, however, require a full parametric model of the task and require some degree of interpretation by an expert viewer who must be present during the scan to determine if they are realistic.

Beyond determining if a subject is actually performing a task, there are a number of other factors that can interfere with the task response. Cognitive effects are chief among them; an IQ of 70 or higher is recommended for a person to reliably perform most task-based fMRI (Morrison, 2010). Various medications may interfere with activation, particularly in certain populations (Neele et al., 2001). Many patients with epilepsy undergo fMRI scans as part of pre-surgical planning, and even brief seizures in the scanner will influence ability to respond to the task.

1.4.3 Signal Drift and Other Sources of Noise

Sources of noise in fMRI are varied and include scanner drift, electronic noise, minor motion artifact, and physiological noise such as breathing and heart

rate (Greve, Brown, Mueller, Glover, and Liu, 2013). Some signal may even come from known networks (Tanaka and Stufflebeam, 2016) but for the sake of task-based fMRI analysis, is still not informative and is therefore effectively noise.

The MRI signal is inherently weak and any loss of signal or added noise therefore has a great effect, especially in fMRI where task-based percent signal change is typically on the order of 3% (DeCharms et al., 2004). Such signal losses and noise may be due to digitization error, electronic noise accumulated in signal transmission from the coil, and magnetic drift or shimming artifacts. Magnetic drift is a gradual change and shift in the magnetic field of the MRI during the scan. Shimming artifacts may be due to slight inconsistencies in the magnetic field that cannot be fully counteracted by the MRI scanner's ability to adjust its main magnetic field, resulting in small regions of different field strength. Or, if the patient moves between the calibration scan and functional scan, the shimming will be ineffective.

1.4.4 Methods of Managing Artifacts and Noise

Various methods have been devised to compensate for the many sources of noise in fMRI, ranging from the simple to the complex. The fMRIB (functional MRI of the Brain) Software Library (FSL) recommends the following pre-processing steps, mostly to remove unwanted signal variance (FSL Course, 2016):

- Motion correction (realignment of each frame to a common frame)
- Slice timing correction
- Spatial filtering
- Temporal filtering
- Global intensity normalization

These pre-processing steps to clean the signal are representative of common steps taken across many pipelines. The spatial filtering is done via convolution with a 3D Gaussian smoothing kernel and increases the statistical power of the GLM, provided the size of the smoothing kernel is less than that of the activated area, by smoothing and effectively averaging out noise. Temporal filtering is straightforward and removes high or low frequencies that are respectively higher and lower than the task frequency. This is founded on the premise that low-frequency drift will be a lower frequency than the task frequency, and that noise is primarily composed of high frequencies. Global intensity normalization is intended to equalize comparison of different scanning sessions or scans from different subjects; different scans will have higher or lower mean signal depending on factors that don't affect the final result, and so this source of variability is removed.

The Human Connectome Project (HCP) (Van Essen et al., 2013) is a large database containing both task and resting-state fMRI data and has developed an advanced processing pipeline to ensure quality results that are free of confounds like motion. A total of 24 motion parameters are regressed from the data before it is processed with the ICA-FIX algorithm. The basis of ICA-FIX is a trained classification algorithm that sorts signal components found with Independent Components Analysis (ICA) as either desired or undesired (Pruim, Mennes, Buitelaar, and Beckmann, 2015). After ICA-FIX, the HCP pipeline includes removal of mean signal and de-trending. In a later pipeline recommended and tested by Siegel in 2016 (Siegel et al. 2016), multiple regressors from white matter, ventricles, and a global brain mask are removed prior to censoring and interpolation between frames affected by sudden motion spikes.

Increased interest in resting state analysis has driven increasingly complex artifact detection and removal methods to be developed, and was likely a large part of the motivation behind the pre-processing pipeline used in the HCP. Wavelet noise de-spiking has been proposed as one method that is motivated by the various types of motion artifacts and how motion affects signals (Patel et al., 2014). Given the range of frequencies described by the authors, wavelet de-spiking would likely clean signals of other kinds of artifacts as well. This method works by transforming time series into the wavelet domain and using the maximum and minimum wavelet coefficients to remove unwanted signal. It is intended to be added on to the end of existing processing pipelines to remove any remaining motion artifact.

1.5 Information Theory in fMRI

The basis of information theory is the quantification and qualification of information content. In this context, information theory is used to distinguish desired task-information from noise and is therefore relevant after discussion of noise sources. Entropy, introduced by Claude Shannon in 1948, is the average amount of information contained in a signal. Entropy as a mathematical formulation existed well before Shannon's work, *A Mathematical Theory of Communication*, but this publication was really the first to introduce it as a concept for signal analysis. This was also the beginning of information theory as a field of study.

1.5.1 Applications of Information Theory in fMRI

Information theory has many applications in identifying and quantizing the information in fMRI signals and noise. There are too many examples to explore all in detail, but some of the most relevant work is discussed here.

Some authors have studied aspects of cognition, such as the latency in time in which information relating to a stimulus reaches different parts of the brain (Alpert, Sun, Handwerker, D'Esposito, and Knight, 2007). Work by Alpert et al. (2008) identified regions of functional specialization in an audio-visual task and the time from the start of the stimulus until different regions became informative of the task. This was found using mutual information, calculated using entropy, and led to creation of a temporal gradient from the primary auditory cortex to higher-order processing regions. It should be mentioned that there are some issues with using fMRI to infer causality and directionality in cognitive functions, largely because of the slow timescale of scanning (on the order of seconds) compared to actual neural signals, but this is nonetheless a fascinating example of applying entropy to neuroimaging.

Using EEG simultaneously with fMRI may help counteract some of the issues surrounding inference in fMRI because of the much faster sampling rate of EEG. Whether there is actually added information from the additional modality, however, is important to know in determining if it's worthwhile to regularly combine both modalities. Information theory, again using mutual information, has been useful in exploring this. One example of this is work by Ostwald et al. using simultaneous EEG and fMRI with a stimulus of high and low contrast checkerboards (Ostwald, Porcaro, and Bagshaw, 2011). Information synergy was calculated using mutual information and entropy to determine the information

content of the joint response distribution and determine if the combined modalities provided more information than either modality alone.

Entropy in different forms has also been used to identify artifacts and even create activation maps in some cases. Most notably, De Araujo used Shannon's entropy to detect activation in event-related fMRI (De Araujo, 2003). Event-related fMRI is where the tasks do not follow a regular block on/off pattern with the task presented for a continuous and pre-set period, but rather are delivered as brief stimuli followed by a relatively extended rest period as compared to block designs. The benefit of applying Shannon's entropy to detect activation in this case is that there are fewer assumptions than a parametric model about the type of response. However, there is one main assumption in De Araujo's work which is that Shannon's entropy is divided into two epochs during and following an event-related stimulus. Use of Shannon's entropy to detect activation was found to be more resistant to low SNR, but it is unclear how well this method would work in block design fMRI tasks. This is due to the assumptions of the epochs of the BOLD response to an event-related stimulus, which differs significantly from block-design.

Some work has intersected study of cognition and functional mapping. Wang et al. used a type of entropy called sample entropy to create expected entropy distributions in the brain (Wang, Childress, and Detre, 2014). Sample entropy is a type of entropy that is often desired for analyzing biological signals because of its sensitivity to self-repetition within signals (for example, cardiac signals). Wang et al. theorized that given the importance of entropy throughout nature, it may have a significant role within the human brain as well. It was shown that there is a sharp change in brain entropy between the neocortex and

the rest of the brain, and that the brain can be organized into different regions of interest (ROI's) corresponding to known functional regions based on mean entropy values. This is important because it suggests that entropy has a highly meaningful role in neural organization and processing. Additionally, Wang et al. hypothesized that task activation would lower regional sample entropy in the brain in areas activated by the task and they were able to show this in a cohort of 16 subjects scanned twice. This demonstrates that entropy can be used to localize task activation in the brain.

1.5.2 Spectral Entropy in fMRI

Spectral entropy is mathematically the same as Shannon's entropy, but instead of being calculated based on probability distributions, it is computed in the frequency domain using the power spectra values of component frequencies. In this sense, spectral entropy is a form of quantifying the amount of frequency information contained in a signal. Signals with few component frequencies or only a single frequency are described as sparse and result in low spectral entropy. On the other hand, signals with many component frequencies (for example, a very noisy signal) will not be sparse and will have very high spectral entropy.

There are many frequencies present in fMRI and there are many ongoing discussions on the roles of different frequencies and how to filter them. For this reason, an application of entropy in the frequency domain is a logical choice. Spectral entropy has been previously used in analyzing neurological signals, such as for monitoring the effect of general anesthesia through EEG recordings

(Vakkur et al., 2004), giving evidence to the relevance of spectral entropy in analyzing neurological signals.

1.6 Regularization

Regularization is the process where some amount of a priori knowledge is used to counteract measurement deficiencies in data. For example, if it is known that the temperature of the body is typically around 37C but that the thermometer being used is very inaccurate, an average of measurements may be made where values further from 37C are given less weight. There is an obvious challenge in data regularization: if the data is regularized too aggressively, it will always return the same result (37C in this example) and will no longer reflect the true measurement. However, there is no benefit to using a regularization scheme if the regularization is too mild.

Regularization has been employed in other cases of functional neuroimaging. One group has used a combined spatio-temporal regularization method to detect functional activation in fMRI (Karahanoğlu, Caballero-Gaudes, Lazeyras, and Van De Ville, 2013). Spatio-temporal regularization refers to a dual regularization scheme with a temporal component that anticipates a block-design in the temporal response of active voxels, and a spatial component that looks for coherent patterns of activation in known predefined regions. The benefit of this method is similar to methods of activation detection using information theory in that it is largely non-parametric and breaks away from assumptions such as timing of task response. It also does not require prior knowledge on the task design. In this particularly example, the combined regularization is suggested as an effective way of studying non-stationary brain dynamics.

In this work, the measurement deficiency is the ability of spectral entropy to detect a sparse signal originating from the fMRI task in the presence of unavoidable fMRI noise. Even when the frequency from the task is clearly dominant in the power spectra, the contributions of noise will increase the spectral entropy – even if each of those contributions are by themselves minor.

1.7 Hypotheses and Objective Measures

The majority of fMRI analysis is currently based on statistical testing of data that has been pre-processed and prepared for optimal analysis. Pre-processing removes some artifacts – or at least, attempts to minimize them – and in cases such as spatial smoothing, is intended to improve statistical power. The statistical analyses used to test the null hypothesis rely on inferences and assumptions about the data, for example the expected haemodynamic response. This analysis leads to the typical activation maps associated with fMRI. The assumptions associated with these maps, such as the expected haemodynamic response (which in fact varies with individuals and brain regions), have led to some work attempting to overcome some of the issues with model-based analysis (Steffener, Tabert, Reuben, and Stern, 2010), but there is still a large need for model-free approaches.

Despite the issues around model assumptions, parametric maps (t-statistic, for example) are still a measure of data quality, albeit one that is far removed from raw signals. Fortunately, there are also known features of fMRI data that can be used to anticipate the quality of the data before statistical analysis and without models. The relative proportions of noise and task in the signal should be in favor of the task, for example, and have good SNR. Some of

these features are relatively easy to mathematically quantify. Slow signal drift can be easily calculated and removed, frequencies over a certain limit are almost certainly noise and can be measured in a Fourier transform. In simulated data sets, the amount of added signal is indicative of the expected final data quality.

Similarly, the number and range of frequencies present is informative of some aspects of the data. Specifically, power spectra that favor the task frequency are likely representative of signals that are rich in useful task information and will lead to increased sparsity of frequencies. This power spectra sparsity can be quantified using information theory in the frequency domain with spectral entropy.

Based on the potential of spectral entropy to quantify information in the frequency domain based on sparsity, and also the large amounts of non-task information contained in all fMRI signals, the following hypotheses are made:

> Hypothesis #1: Data-driven regularization will improve the ability of spectral entropy to detect useful task-related information.
>
> Hypothesis #2: Spectral entropy will correlate to known factors that relate to the amount of useful information in fMRI signals, particularly when combined with regularization.

Objective measures to test and study the first hypothesis, that data-driven regularization will improve the ability of spectral entropy to detect task-related information, included the change in spectral entropy on idealized signals before and after regularization, and the change of spectral entropy's relationship to t-statistic (founding using parametric models) and percent signal change before and after regularization.

Objective measures for the second hypothesis regarding the relationship of spectral entropy to information content were the spectral entropy would correlate to SNR in idealized signals, t-statistic in both simulated and real datasets, and to the amount of added signal in simulations.

A secondary but closely related hypothesis is that, given the above hypotheses and objective measures, regularized spectral entropy will produce meaningful maps that reflect known activation in fMRI scans. Additionally, based on the evidence for replicable consistent distributions of other forms of entropy (Wang, Childress, and Detre, 2014), it is hypothesized that spectral entropy (regularized or not) will show consistent and repeatable distributions across subjects.

These hypotheses and related objective measures are intended to help approach fMRI data from a more fundamental standpoint than current statistical testing and parametric models. Being able to measure data quality before taking it offline and performing extensive pre-processing and statistical analysis is currently not feasible on most modern MRI scanners, and this method works without an assumed haemodynamic response model. While this work does not yet claim to be an optimal method for real-time analysis of fMRI data quality, it is intended to be part of a broader body of work moving in the direction of improved fMRI data quality metrics.

Chapter 2: Theory of Functional MRI and Entropy

There are many types of MRI scans with different purposes and types of contrast. fMRI, however, is particularly special because it can reveal how the brain works and where functional regions exist in the central nervous system. The basis of fMRI is the BOLD contrast. When repeated in time, this contrast (usually in response to a stimuli) can be used to identify functional regions by the change in CBV.

2.1 Magnetic Resonance

Medical magnetic resonance almost entirely relies on the proton: a spin ½ atom that is fortunately plentiful in the body. A large magnetic field (often called the **B-field**) is always present along the axis of the bore of the magnet. The spins of protons align either parallel or anti-parallel to this magnetic field; parallel results in a slightly lower energy state. The difference of these energy state is given by

$$\Delta E = -\gamma \cdot m \cdot \hbar \cdot B \qquad 2.1$$

Where B is the magnetic field strength of the B-field and is a function of position, γ is the gyromagnetic ratio, m is the spin ($1/2$ in the case of a proton), and $\hbar$ is the reduced Planck's constant (Planck's constant divided by 2π).

Field gradients, much smaller than the B-field, are used to adjust the local magnetic field and give rise to the specific frequency of each proton's spin. This is called the Larmor frequency and is given by the following:

$$\omega = -\gamma \cdot B \qquad 2.2$$

Where γ is, again, the gyromagnetic ratio of the particle. The Larmor frequency is necessary for magnetic resonance: energy can only be transmitted to the spins if

the frequency is that of the Larmor frequency. This allows specific slices of tissue to respond to the radiofrequency (RF) pulses.

2.2 Blood Oxygen Level Dependent Signal

As mentioned above, the BOLD signal is at the heart of fMRI. It is a physiological response caused by the metabolic requirements of firing neurons, and is therefore closely related to neural activity and cognitive processes.

2.2.1 Biophysiological Origin

NVC (sometimes called cerebro-vascular) is the process in which blood volume fluctuates in response the metabolic activity of neurons. The process is not entirely understood, but results from synaptic activity and neuronal activation leading to increased energy use by neurons and astrocytes. Increased local glucose and oxygen consumption leads to dilation of nearby blood vessels through complicated action of vasoactive chemicals (Iadecola and Nedergaard, 2007; Attwell et al., 2010). Neurons stimulated by a task therefore have increased metabolic activity and give rise to increased local CBV.

The obvious drawback to the biophysiological origin of the fMRI signal is that is an indirect measure of neural activity. Any factor influencing the NVC or even blood oxygenation will influence the results of an fMRI scan. Important factors to consider are pathologies like tumors or long-established epilepsy, or medications and neuropsychological effects such as the patient's ability to do the task. Pre-existing familiarity with the task or task-blocks that are too long will also result in "conditioning" of the haemodynamic response where the effect will be decreased (Henson and Rugg, 2003; Soon, Venkatraman, and Chee, 2003; Sagaert, Weber, Petersson, and Hagoort, 2013).

2.2.2 Magnetism of Oxygenated/De-oxygenated Blood

Oxygenated haemoglobin is diamagnetic (repelled by a magnetic field) while deoxygenated haemoglobin is weakly paramagnetic (drawn to a magnetic field) (Bren, Eisenberg, and Gray, 2015). The paramagnetic nature of deoxygenated haemoglobin locally distorts the magnetic field of the MRI, and therefore oxygenated haemoglobin results in an increased T_2^* value and an increased signal in a T_2^* weighted scan. As a combined result of NVC, neural metabolic activity and the difference in magnetic properties of oxygenated and deoxygenated haemoglobin, signal increases in brain regions used in a task.

2.3 Task Design

The design of an fMRI task is referred to as the *paradigm*, and in most cases is a block design (sometimes called boxcar design) because of its consistently alternating task and contrast pattern. A diagram and example is included in figure 2.1.

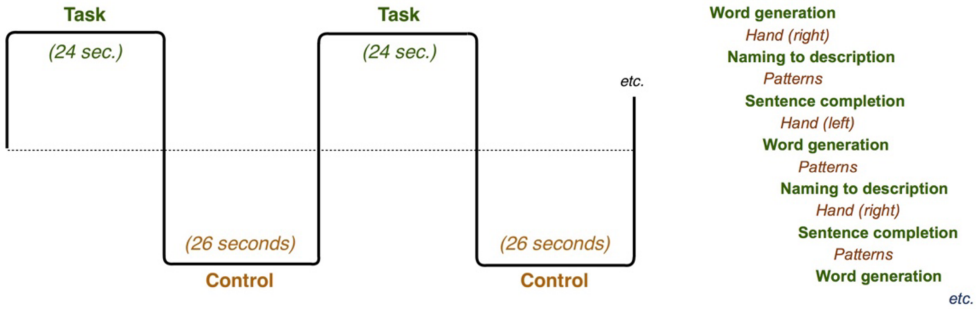

Figure 2.1 Diagram of task and control in a block design fMRI experiment (left), and examples of alternating task and control tasks in a language experiment (right). This paradigm is based off of the work of Barnett, Marty-Dugas, & McAndrews (2014) which was further developed by O'Grady and Omisade (2016).

Block design is by far the most common method for clinical fMRI because of its simplicity and robustness in being processed using the GLM. The design is

simple: the task blocks activate the desired regions of the brain, and the contrast blocks activate all other regions activated in the task blocks except those desired in the task. For example, a language task may involve filling in the blanks in incomplete sentences. (Barnett, Marty-Dugas, & McAndrews, 2014) The contrast could be identification of patterns by reading left to right. This contrast will activate regions involved in visual processing in a way similar to reading but will not involve language regions.

2.3.1 Motor Tasks

Motor tasks are used to identify the motor and pre-motor cortex in the brain and are among the most robust types of fMRI scans (Yousry et al., 1995). This is likely mostly due to the simplicity of the task: no complex cognitive demands that would recruit many brain regions are required for basic motor control. In fact, finger tapping was the first true fMRI experiment performed in 1992 by Peter Bandettini. Motor mapping usually relies on finger tapping, either sequential fingers in repetition or in a predefined order, but may also involve the tongue, foot, or other body parts.

Closely related to motor mapping is sensory mapping. Instead of performing a physical motion, the patient will be physically stimulated by an external source, such as the motion of toothbrush against the skin. This activates regions in the sensory cortex that can then be used to trace where sensations from different places are initially processed in the brain.

2.3.2 Language Tasks

Language tasks are more complex than motor because of the greater cognitive resources needed and increased location variability of canonical

language areas. Because language tasks may inadvertently recruit multiple aspects of cognition - working memory, visual processing, even motor cortices due to thinking about how to sound out words – contrasting out non-language regions requires more sophistication. For example, reading of text should be contrasted with pattern identification, or listening to spoken words should be contrasted to unintelligible words. Similarly, authors recommend a combination of different task types to best focus activation on canonical regions (Gaillard et al., 2004).

These so-called canonical regions are Broca's area in the inferior frontal cortex and Wernicke's area in superior-posterior temporal lobe adjacent to the angular gyrus and inferior to the supramarginal gyrus (Binder et al., 1997). Broca's area is primarily responsible for expressive language (i.e., creation of speech), and Wernicke's is primarily responsible for receptive language (i.e., understanding speech) (Müller et al., 1997). In 95% of right-handed individuals and at least 60% of left handed individuals, language is entirely in the left-brain hemisphere (Isaaks, Barr, Nelson, and Devinsky, 2006). In the remainder, it is either in the right-hemisphere or divided bilaterally. This is especially common in populations with long standing pathology, such as those who have had epilepsy since a young age, or a slow growing brain tumor. Such pathology may interfere with normal brain language lateralization that occurs in childhood resulting in atypical distribution and increased need to correctly identify laterality for potentially curative surgery that does not result in large functional losses (Hamberger and Cole, 2011).

2.4 fMRI Analysis

There are two broad categories of fMRI analysis: parametric and non-parametric. Both have benefits and deficits, and the choice of processing is circumstance dependent.

2.4.1 Parametric fMRI Analysis

The most common method of parametric fMRI analysis is the GLM, the basis of which is an "ideal" function: the convolution of the task timing with the haemodynamic response function. The haemodynamic response is the supposed response of CBV in response to neuronal activity and its exact function may vary depending on software choice, but the gamma function is a common example. An example of a haemodynamic response, the task-timing diagram, and the ideal function is given in figure 2.2.

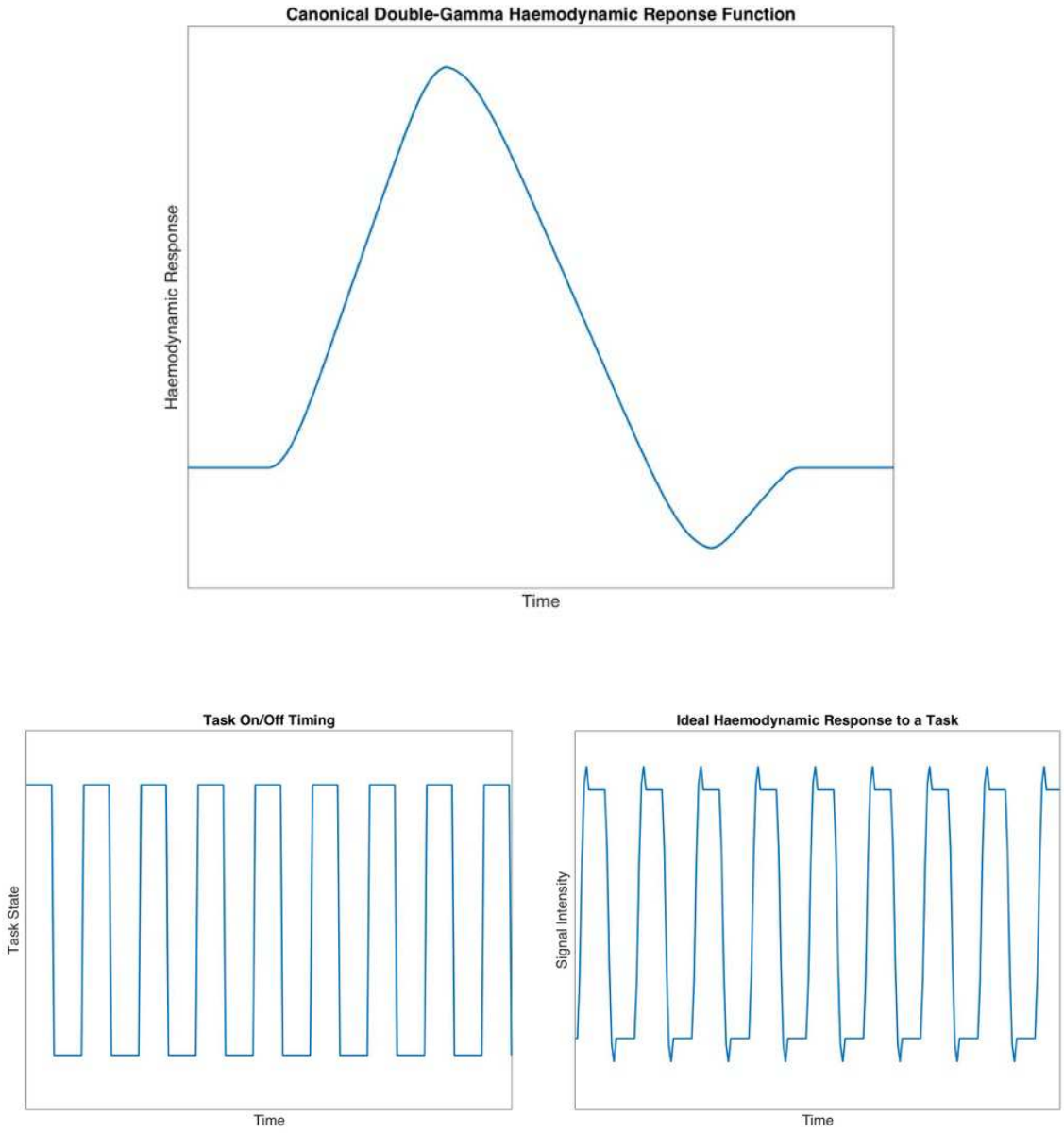

Figure 2.2 The canonical double-gamma haemodynamic response function, the assumed response of CBV to a task (top). Bottom left: task timing diagram. Bottom right: the "ideal" response to the task, which is a convolution of the haemodynamic response function and the task timing function.

The actual signal from each voxel is modelled as a weighted sum of the ideal response, the average signal intensity, signal drift, and noise. Weights are produced by a least squares fit.

The final activation map is, therefore, a map of how well the idealized response fits the real signal. This can be given by a t-test (the author's preferred method) or an F-test. A t-value is calculated by dividing the regression parameter for a voxel and its sample standard deviation estimate:

$$t = \frac{b_i}{\sigma(b_i)} \qquad 2.3$$

Where $b_i$are the weights of the least squares fit to the model, and $\sigma(b_i)$ is the sample standard deviation of the estimates of the fits.

2.4.2 Non-parametric Analysis

One potential downside of parametric analysis is that the model assumptions are most sensitive to information that fits the model in spite of the fact that other information may still be valuable. This other information might include areas de-activated by the task due to haemodynamic suppression, regions activated that have different haemodynamic responses than the classically assumed response, or regions with different latencies. Another is that they require large amounts of a priori information, such as the shape of the haemodynamic response. Some clinical centers will actually shift the ideal function temporally to best match the latency of the haemodynamic response of individual patients: this is an example of additional a priori information being used to maximize the output of a model that is designed to respond only to one particular aspect of the data. It is also an example of latency in task response that varies between individuals.

Alternative analysis methods for task-based fMRI have emerged but are not widely used. They benefit from less a priori information, but also do not focus in on the task information as rapidly. Independent components analysis

(ICA) is used in fMRI but may reveal a plethora of signal sources that range from real brain networks to noise; activation in desired areas due to the task will be contained in one or more of these.

2.5 Entropy and Information Theory

Since Shannon's publication, Information Theory has expanded greatly and so have the definitions and types of entropy and related quantities. It is important to note that the basic definition of entropy remains the same, but the "flavour" changes with different formulations. Briefly, different kinds of entropy measure different aspects or kinds of average information content. Some of the most relevant types of entropy are discussed in the following subsections, as well as some other key concepts in Information Theory that are found in the neuroimaging literature.

It is important to always remember the common definition of entropy, the expected amount of information content. When the outcome of a measurement, such as at a particular time point in a signal, is known and certain, the entropy will be zero. Conversely, if each measurement has a different or less predictable outcome, there will be non-zero entropy. Therefore, a signal that is flat (uniform value) would have zero entropy, while one that is random or varied at different points in time would necessarily have non-zero entropy.

2.5.1 Different Forms of Entropy in Neuroimaging

Shannon's entropy is likely the most "generic" form of entropy and is calculated using probability distributions of different states. These may be various types of states; in neuroimaging signals they might be signal intensity values, for example. The dependence of entropy on probability is how the

expected amount of information content is derived. With each new measurement of a signal value, the probability of finding the signal in that state is measured. If every measurement gave the same result, the probability of that result would be 100% and the expected information content low and corresponding entropy low. Conversely, if the signal had equal probability of being in many different states, the average information content would be high and so would the entropy. The reliance on probability densities has some inherent challenges in neuroimaging because the accuracy of the probability estimate is limited by the number of sample points (Ostwald and Bagshaw, 2011). This is an issue that while often ignored in neuroimaging work using Shannon's entropy, is now becoming more frequently discussed.

In addition to the standard form of Shannon's entropy, sample entropy and approximate entropy are found in the context of neuroimaging. Approximate entropy measures the degree of regularity or predictability in a time series or signal, and was originally created for use in analyzing medical signals (Pincus, Gladstone, and Ehrenkranz, 1991). It is a measure of how likely a pattern or patterns will be proceeded by a similar pattern or patterns. A signal with many repeating patterns will have low approximate entropy, a signal with few repeating patterns (and therefore low predictability and regularity) will have high approximate entropy.

Sample entropy is a modified form of approximate entropy. The benefit of sample entropy over its predecessor is data length independence, as well as no internal self-comparison. Both forms of entropy use templates, smaller samples of the entire time series, of length m and $m+1$. The distance between templates of

the same length is compared and those distances that are less than a pre-determined distance *r* are counted and used in the following formula:

$$Sample\ Entropy = -\log\left(\frac{A}{B}\right) \qquad 2.4$$

where A is the number of template vector pairs of length *m+1* with distance less than *r,* and B are those of length *m* with distance less than *r.*

Spectral entropy is a variation on Shannon's entropy and is the main method used in this work. Probability densities are replaced with power spectra values, and the information content measured is actually the richness of frequency content in the signal. A sine wave would therefore have zero entropy: there is only one frequency present. A noisy signal, however, would contain a great deal of frequency information and have relatively high spectral entropy.

It would be possible to use other measures of entropy in the frequency domain to achieve a similar purpose as regularized spectral entropy in this work. For example, Gini entropy could be employed to identify sparsity of frequency distribution. In this work, Spectral Entropy was chosen because of existing demonstrations of its utility in analyzing neurological signals, as well as its efficient calculation method.

2.5.2 Other Key Concepts in Information Theory

Entropy is the most commonly referenced aspect of Information Theory in neuroimaging, but several other concepts are also used frequently. Conditional entropy is the entropy of a signal after the variability due to another signal is accounted for (i.e., the conditional entropy H(X|Y) is the entropy of X after the variability attributed to Y is removed).

Mutual information is probably the most important concept in Information theory after entropy. Mutual information is a measure of statistical non-independence between signals. It is given by the difference of the entropy of a signal and its conditional entropy with another signal. Mutual information has found uses in studying the transfer of information between different parts of the brain (Alpert, Hein, Tsai, Naumer, and Knight, 2008), or between fMRI signals and stimuli as a way of determining which voxels are responding to a task (Tedeschi et al., 2005).

Chapter 3: Experimental Details

Development of spectral entropy and regularization used both real and simulated data; noise parameters in the simulated data were informed by real data sets such that the power spectra were matched. Given the importance of the simulated data sets, these are discussed in more detail in the following section.

3.1 Simulated fMRI Data

Simulated data was created using the NeuRosim software package written in R (Welvaert, Durnez, Moerkerke, Verdoolaege, and Rosseel, 2011). Datasets were based on the MNI152 brain with 2x2x2mm resolution (Mazziotta, Toga, Evans, Fox, and Lancaster, 1995), and 100 frames (TR's) of TR = 2s. Activation was added in a block pattern with block size of 20 seconds.

3.1.1 Derivation of Parameters Based on Real Data Spectra

Spectral entropy relies on detection of frequencies and thus, accurate representation of frequency distributions is critical. The following noise parameters were adjusted as follows:

- Autocorrelation
- White noise
- Physiological noise (heart rate, breathing)

Power spectra in groups of random voxels were sampled and compared to real data sets' power spectra. Additionally, averages of the whole brain power spectra in simulations were ensured to be highly similar to those of real data. Example power signals and power spectra are shown in figure 3.1. Details on the real data collected are discussed later.

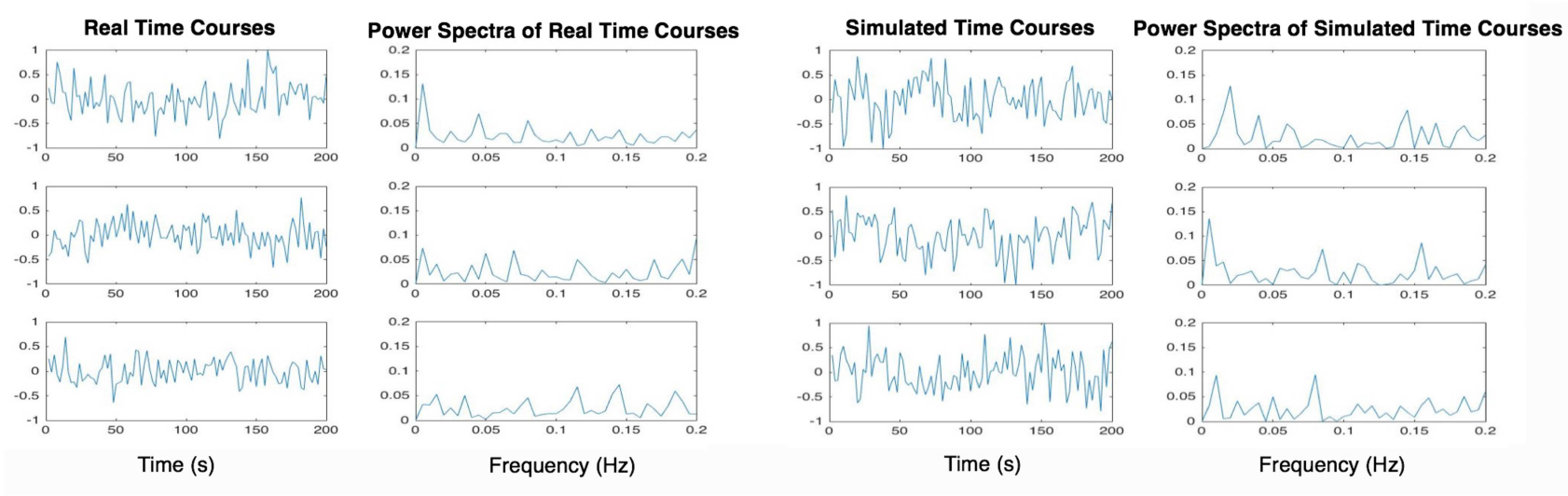

Figure 3.1 Comparison of three example signals and their power spectra from simulated data sets and the real data set used to inform parameters in the simulated data set

3.1.2 Region of Added Activation

Recognizing that for the purposes of spectral entropy the location of the added activation should be irrelevant, an easily identifiable spherical ROI in the right motor cortex was selected of size 11.04cm^3 (1380 voxels). Similarly, because of the size of activation varies in real fMRI data, the exact size of activation in the simulations was not considered highly important as long as it was reasonable with regards to normal areas of activation seen and typical sizes of real functional regions in the brain. The region of added activation is shown in figure 3.2.

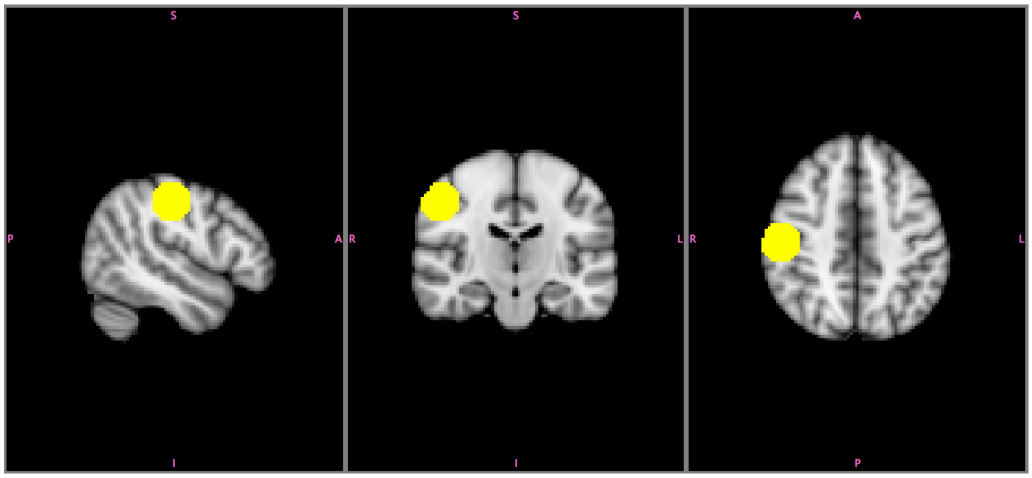

Figure 3.2 Area of added activation, located in approximately the right motor cortex, in simulated data sets, overlaid on the MNI152 standard brain.

3.1.3 Effect Size and Percent Signal Change

Because of the nature of the simulated data, percent signal change was a convenient way to calculate and track the degree of added activation in the ROI. Percent signal change was chosen to range between 2% and 5% as a reasonable range observed in real data (DeCharms et al., 2004). Percent signal change is rarely used in current fMRI analysis, however; the preferred method is to produce a t-statistic map using the General Linear Model (GLM) to demonstrate

activation. As mentioned earlier, however, when adding activation to a simulation, percent signal change is an obvious way of quantifying the amount of added activation.

In the NeuRosim coding environment, the amount of added activation was actually given by *effect size*. Percent signal change as a function of effect size is given as follows:

$$PSC = \frac{100 * Effect\ Size}{Mean\ Resting\ Signal} \qquad 3.1$$

In this case, the mean resting signal was taken from a resting state simulation with the same noise parameters and was found to be 5936.64.

3.2 Real fMRI Data

Real data used to inform noise parameters in the simulations was collected on a General Electric 3-Tesla MR750 Discovery MRI using an echo-planar imaging sequence with the following parameters: in-plane resolution 1.72x1.72mm, slice thickness 3mm, TR = 2s, TE = 25ms, flip angle of 77 degrees, and 48 axial slices. An anatomical scan was included for registration of the functional scan and localization of the activated regions. This was a T1 weighted spoiled gradient echo sequence with isotropic resolution of 1x1x1mm^3, TR = 5.7ms, TE =2.1ms, field of view = 22.4cm, flip angle of 12 degrees, and 168 axial slices. Acquisition time for the anatomical scans were approximately 5 minutes. Subject data was collected with informed consent and Nova Scotia Heath Authority Research Ethics Board approval, using an integrated fMRI language paradigm.

The language scan included three tasks: word generation to a presented letter, generating the missing word at the end of incomplete sentences, and

naming items or concepts described by a sentence. Contrast included scanning two patterns on either side of a fixation cross to determine if the patterns were the same, and alternating finger tapping. The latter contrast is intended to mimic the visual effect of reading a sentence, while the former counteracts any unintended motion induced by thinking of speech or motion-related words.

There were a total of 9 task blocks of length 24 seconds and 8 contrast blocks with length of 24 seconds. Before each block, a 1-second warning was displayed for both contrast and task to "prime" the subject of the incoming stimulus. The total paradigm length, including a warmup time of 6 TR's, was 7 minutes and 12 seconds.

3.3 Spectral Entropy Pre-processing

In this work, spectral entropy and the combined regularization are intended to be applied to essentially raw data – signals that have been at most only minimally modified. However, to speed up calculation some pre-processing steps were included. These include removal of non-brain tissue, such as the skull. Spectral entropy distributions of non-brain tissue are not informative of the scan quality and may even be misleading should they provide non-relevant information. Furthermore, reducing the number of signals to process makes the spectral entropy and regularization calculations faster.

Basic motion realignment was also used, where each image volume was spatially translated and/or rotated to match the original. This is standard pre-processing for all fMRI, and ensures that the time course from each voxel is actually representative of its true signal (i.e. instead of being a combination of neighboring voxels). Motion is unavoidable in fMRI, and happens in varying

degrees. A low-motion scan will have very slight and gradual motion, perhaps on order of a few millimeters or degrees between the first volume and the last volume. A high-motion scan will have more abrupt and likely larger motion. Motion realignment will counteract the effect of normal gradual motion but will not correct artifacts due to larger motion which typically manifest as signal spikes. For larger motion, correction methods typically motion regress 12 or more motion parameters, such as the 24 parameters used to ensure data quality in the HCP (Siegel et al., 2016). Motion realignment is considered a reasonable pre-processing step in this case as it does not remove artifacts from larger motion parameters (and therefore accurately reflects all aspects influencing fMRI data) but does not allow the data to be unnecessarily interpreted as low quality due to normal gradual motion.

3.4 Spectral Entropy Calculation

Shannon's entropy is given by the following:

$$H_{Shannon} = -\sum_i P_i \log(P_i) / \log(N) \qquad 3.2$$

where P_i are probability densities for particular states and N is the total number of states. These probability densities are calculated from real data distributions and are therefore subject to some estimation error that has until recently, been only minimally addressed in applications of entropy to neuroimaging. In frequency space, this problem is circumvented because the probability densities become power spectra values. Spectral entropy is therefore given by the following:

$$H_{Spectral} = -\sum_i F_i \log(F_i) / \log(N) \qquad 3.3$$

Here, F_i refers to the power of a given frequency i. To produce the power spectra, a fast Fourier transform (FFT) is used and the resulting complex values are multiplied by their conjugate and normalized. The frequencies of the power spectra are set between 0 and 0.2Hz in increments of 0.005Hz. This range was chosen to reflect a reasonable range of frequencies that might be expected in an fMRI signal (DeCharms et al., 2004) and also to accommodate the range of frequencies that could be detected in a typical fMRI scan of approximate length 5-10 minutes (for example, a very low drift frequency may not be detected in a scan of only 5 minutes). Additionally, the frequencies are always resampled at this same range to ensure equal comparison of any scans of different length. The division by log(N) in the calculation of spectral entropy ensures that the value varies between 0 and 1, where 0 indicates absolute sparsity of the signal and the limiting case of a sine wave where only one frequency is present, and 1 is high entropy where many frequencies cohabit the signal.

3.5 Regularization

Because of the variety of frequencies always present in fMRI, even a signal that is full of task-related information content may have a high spectral entropy value. This is because spectral entropy will respond to the overall amount of information in the frequency domain and many sources of noise (or noise frequencies) will contribute a significant amount of information even if each component is by itself small. Much of this noise is not only expected but is also impossible to eliminate, such as physiological noise.

To counteract this (i.e., have spectral entropy produce a value that meaningfully represents when frequency content is sparse and in favor of the

task), a data-driven regularization scheme for an ill-fitted problem is used. Filtering methods were initially tested but not used because of the inability to be data-driven and because if used too aggressively, can produce sparse frequency spectra inappropriately. The regularization method used was based upon the differences of power spectra values and tuned using simulations with known parameters to optimize the ability of spectral entropy to respond to the amount of task-based information content in the signal.

To achieve this, Tikhonov regularization was used (Tikhonov, 1963) and is given by the following formulae:

$$\|Ax - b\|^2 + \|\Gamma x\|^2 \qquad 3.4$$

with the solution of:

$$x = (A^T A + \Gamma^T \Gamma)^{-1} A^T b \qquad 3.5$$

where b is a vector of absolute difference values of each frequency's power from that of the task in the case of perfectly sparse power spectra representing the task paradigm (i.e., if the 3rd frequency was that of the task, b = [1 1 0 1 …1]). The matrix **A** is the identity matrix **I** multiplied by the actual differences of task frequency power to all other frequencies (i.e. A_{11} is the absolute difference of power of the first frequency and the task frequency). Lastly, Γ is the identity matrix multiplied by a constant α, where smaller values result in stronger regularization.

The final power spectrum is the regularization solution x multiplied by the original power spectrum. This power spectrum is then renormalized.

3.6 Calculation of Sample Entropy

This work is about the application of spectral entropy and data regularization to determine the presence of task related information in an fMRI scan. However, another method of detecting activate regions was proposed by Wang et al. using sample entropy (Wang, Childress, and Detre, 2014).

In the work by Wang et al., 16 subjects completed task scans twice to create 32 task data sets. The same subjects also completed 2 resting state scans. Wang et al. demonstrated that there is a decrease in sample entropy in a region activated by the task by subtracting each subject's task scan sample entropy map from a corresponding resting state scan sample entropy map and computing a two-sample Student's t-test on the differences. The t-statistic values were seen to correspond with a GLM group map of the area activated.

To replicate this in a way that sensitivity and specificity could be compared to spectral entropy methods, 32 simulations were created with 8 percent signal change values again varying between 2% and 5% (4 sets of each percent signal change were made). To avoid redundant data, a single resting state simulation was created. Sample entropy maps of all task scans and the resting state scan were creating using Wang et al.'s method, and differences were calculated between voxels in the task scan sample entropy maps compared to randomly chosen voxels in the single resting state sample entropy map. A key assumption is that in simulated resting state data sets, there should be no average difference of any kind of entropy between different groups of voxels (or a different simulated resting state scan with the same parameters).

Specificity and sensitivity, found taking the best possible combination of both, were compared for the sample entropy map as well as the spectral entropy maps and traditional GLM maps for each of the 32 simulated data sets.

Chapter 4: Data-driven Regularization to Improve Spectral Entropy Characterization of fMRI Data

The first hypothesis in this work was that data regularization would improve the power of spectral entropy in detecting useful task-related information. In this context, "task-related" may refer to an active task (such as a language or motor task), or sensory stimulation, or other stimuli that is provided in block-design format in lieu of a task that is performed by the subject. The reasoning for the hypothesis about data regularization is due to the large number of noise sources in the signal; even a very good scan still has sources of noise or information interfering with the desired data. Regularization is useful for extracting information when there is some other known a priori information present.

In block-designed fMRI, one core piece of known information is the frequency of the task signal. A goal in this work was to remain as non-parametric as possible in the interest of only handling raw, unprocessed or minimally processed signals, so only the frequency of the task being completed is taken as input for the regularization scheme. In this work, Tikhonov regularization was chosen because of its prior applications in MRI, such as for image reconstruction (Ling, Xu, & Liang, 2004).

4.1 Effect of Inherent fMRI Noise on Spectral Entropy

It cannot be over-emphasized that there are many sources of noise in fMRI. These contribute to non-sparse frequency spectra. In an ideal signal, found via the convolution of the haemodynamic response and the task function, there is one very dominant frequency – that of the task. In a strong signal, as shown in

figure 4.1, this frequency will still be dominant but other frequencies still contribute. Subjectively, this is a sparse signal – or at least, may be argued to be a sparse signal - favoring the task frequency. However, because of the many component frequencies and the normalization involved in the spectral entropy calculation, this results in a high value of spectral entropy. When there are many frequencies present in a power spectrum, even if they are all relatively small, their joint contribution will result in a high value of entropy. Even if a power spectrum is dominated by one single frequency, the entropy may still be high because there are other frequencies with low power but in great quantity. This is illustrated in figure 4.1:

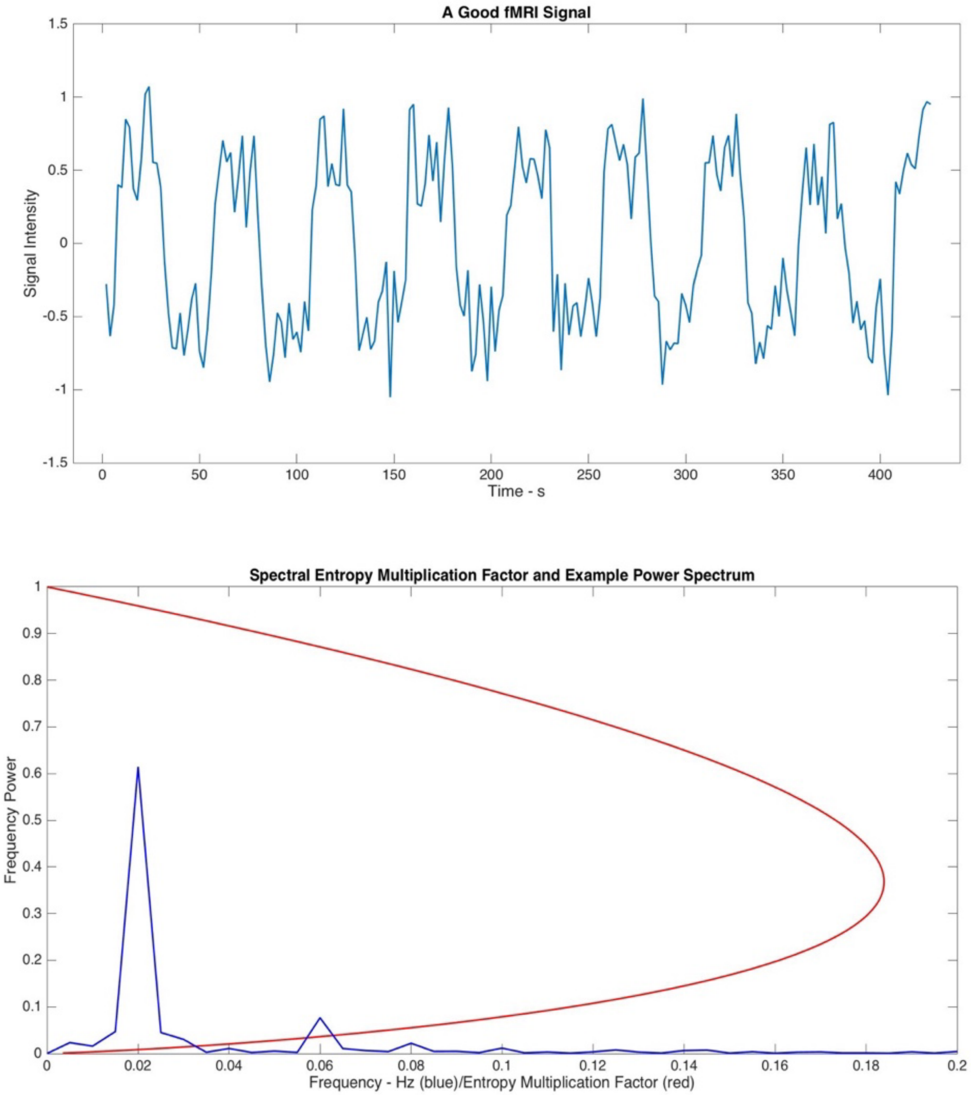

Figure 4.1 (top) A "strong" fMRI signal showing clear response to a task. (bottom) The power spectrum for the signal on top is shown in blue, and all values of spectral entropy are shown in red (i.e. $Spectral\ Entropy = \sum_i F_i \log(F_i)$ *for all F between 0 and 1). Normally, the values in the red curve would be appropriately normalized. However in this case they are multiplied by an arbitrary factor for illustration with the power spectrum. The strong peak at 0.02Hz in the blue power spectrum will result in a relatively high spectral entropy value because of the noise. In this case, a low spectral entropy value is desired to represent the relative frequency sparsity of the signal.*

It is always expected that many frequencies will be present, and so in many cases these are removed with standard preprocessing. Some authors completely remove all low frequencies because this information will only relate to magnetic field drift and other artifacts (Smith et al., 1999). In resting state fMRI, frequency filtering is a necessary standard step to remove noise and unwanted signal, and a typical bandpass range is 0.01-0.08Hz (Chao-Gan and Yu-Feng, 2010).

Extensive filtering would not be a good solution to regularize spectral entropy and reduce the effects of many noise frequencies, however. If all frequencies outside the task frequency were removed and the power spectrum was renormalized as is necessary for spectral entropy calculations, the task frequency would always dominate. The goal of spectral entropy is to determine when the power spectrum is sparse in favor of the task frequency: if the noise is greater than the task frequency, this should be reflected by the entropy. Even careful filtering carries the risk of obscuring the true relationship of noise and useful signal. This situation presents a unique opportunity for data-driven regularization.

4.2 Data-Driven Regularization for an Ill-posed Problem

The regularization scheme should be data-driven in the sense that it must discriminate when the signal is clearly sparse and in favor of the task frequency, and only then increase the power spectrum sparsity and in turn, decrease the spectral entropy. In other words, if the task frequency is dominating the noise frequencies, the regularization should be stronger. Thus, the regularization

should be based upon the difference of the task-frequency to other frequencies. In this sense, it is an ill-fitting problem as there is no one perfect solution.

This regularization is ensured to be data-driven in the sense that it is based upon the actual differences of task frequency to other frequencies. This is an inherent and necessary part of the regularization method; the change made to the data will vary with the data itself in a way that is useful for spectral entropy. Figure 4.2 illustrates this effect, wherein the relative height of the task frequency alters the effect of the regularization.

The regularization is designed to make subjectively sparse power spectra objectively sparse according to spectral entropy. If it is clear to an observer that the task frequency is dominating the signal, the regularization will accentuate this in such a way that entropy will then decrease and reflect the fact that the signal is sparse in overall frequency information but rich in task-related information.

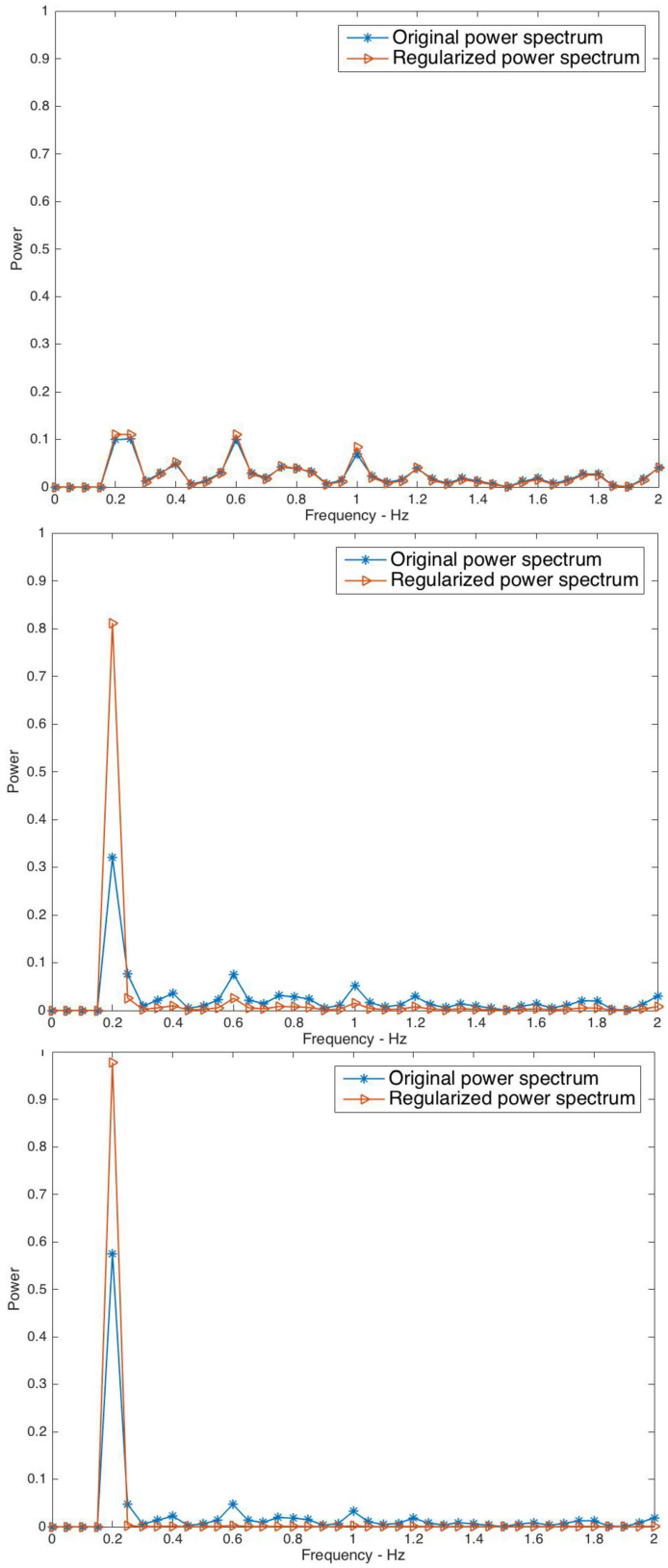

Figure 4.2 The effect of regularization increases with the difference of the task frequency to all other frequencies. Original power spectra are shown in blue, regularized power spectra are in red. On the top, the task frequency power is comparable to the other frequencies' powers and the regularization has little effect. On the bottom, the task frequency dominates the power spectra and the regularization exaggerates this effect.

In these examples, a value of 0.07 was taken for the regularization parameter.

4.3 Role of Synthetic fMRI Data

Determination of the constant α, introduced in chapter 3, is critical in balancing the efficacy of the algorithm while staying true to the data. The goal of this work was to detect when task frequencies were present and make significant contributions to the power spectrum, assuming these frequencies would most likely be due to the performance of the fMRI task by the patient. Simulated data proved invaluable for this, as the implicit goal was to detect voxels activated by the fMRI stimulus. Unlike in real data, activated areas are known in simulated data. This allows calculation of sensitivity and specificity for any method of detecting active voxels.

4.3.1 Sensitivity and Specificity

Sensitivity and specificity are extremely useful measures in medicine and science. They are calculated using true positive, true negative, false positive and false negative rates. In this case, true positive values are those with low spectral entropy that fall within the ROI of added activation. True negative values are those with high spectral entropy and outside the ROI of added activation, false positive values are those with low spectral entropy outside the ROI of added activation, and false negative values are those with high spectral entropy within the ROI of added activation.

Sensitivity is also referred to as the true positive rate, and gives the fraction of truly active voxels that were identified as such. Specificity is analogous to sensitivity for true negatives in that it is the fraction of truly negative voxels identified as such. Specificity is also called the true negative rate. These are given in the following formulae:

$$TPR = \frac{TP}{TP + FN} \quad 4.1$$

$$TNR = \frac{TN}{TN + FP} \quad 4.2$$

Where TP and TN refer to true positive and true negative, and FP and FN refer to false positive and false negative.

4.3.2 Degree of Added Activation

The choice of activation strength (given as either effect size or equivalently, percent signal change) can be completely controlled in simulated data. In keeping with the choice of realistic noise parameters for the simulated data, it is logical to use realistic amounts of added signal change for development of the regularization scheme. The choice of percent signal change was chosen to be between 2%-5% (DeCharms et al., 2004).

It's important to address the fact that the precise values of percent signal change are less important than choosing a reasonable range of values. The amount of added activation in real fMRI data sets will vary considerably and depends on many technological to bio physiological factors. Even within a single dataset there will be a range of signal change within different parts of the brain. The main concern in choosing the range of added activation in the simulated datasets was therefore to represent realistic values while acknowledging that exact values will vary greatly in reality.

4.4 Determination of Regularization Parameters Using Simulated Data

The regularization parameter to be determined, α, becomes excessively strong as it approaches a value of 0 and increasingly ineffective as it becomes larger. For perspective, a value of 0.00001 will result in severe over-

regularization where the power spectrum will be distorted from reality, while a value of 0.3 will barely effect the power spectrum.

Here, the value of α was varied between 0.005 (aggressive regularization) and 0.15 (light regularization) in steps of 0.01. Once maps of regularized spectral entropy were created for each activation size and value of α, the threshold cutoff that optimized sensitivity and specificity was calculated. In the absence of an obvious way to threshold the spectral entropy, the best possible threshold was taken as an available data-driven method. To minimize the number of variables from four (percent signal change, α, sensitivity, and specificity), sensitivity and specificity were combined to be the distance to the top left corner in the Receiver-Operator Characteristic (ROC) curve:

$$distance = \sqrt{(1 - sensitivity)^2 + (1 - specificity)^2} \qquad 4.3$$

This relies on an assumption that this distance is equivalent to optimizing both values simultaneously as much as possible. To counteract the fact that lower percent signal changes will have greater distances overall because smaller amounts of added signal will make detection of task information inherently difficult, the mean distance from each percent signal change was subtracted.

Reduction of the number of variables from four to three (sensitivity and specificity were combined into "distance to the top left corner of the ROC") allowed optimization of α across different amounts of percent signal change. Two factors were considered: minimization of the mean distance, and variation in distance values across different percent signal changes. The latter was considered important as the regularization should perform similarly for different

levels of realistic activation. These values were weighted equally in the selection of α and the cost function used is given here:

$$Cost\ function = 0.5 * Dist(\alpha) + 0.5 * STD(\alpha) \qquad 4.4$$

Where *Dist* is the distance to the top left corner of the ROC plot (the vertical axis in figure 4.3 below), and STD is the standard deviation of these distances for each value of α. In total, 48 datasets were used to optimize the regularization parameter (6 replications with varying noise of datasets with 8 levels of percent change). Regularized spectral entropy maps with regularization parameters of 0.005, 0.015, 0.025, 0.035, 0.045, 0.055, 0.065, 0.075, 0.085, 0.095, 0.105, 0.115, 0.125, 0.135, and 0.145 were produced, giving a total of 720 maps.

A plot of the distance to the top left corner of the ROC curve (sensitivity and specificity) as a function of percent signal change and α can be seen in figure 4.3, with accompanying error. In this plot, effect sizes were resampled to 30 values between 2-5%, and alpha values resampled to a resolution of 0.001 (141 values between 0.005 and 0.145).

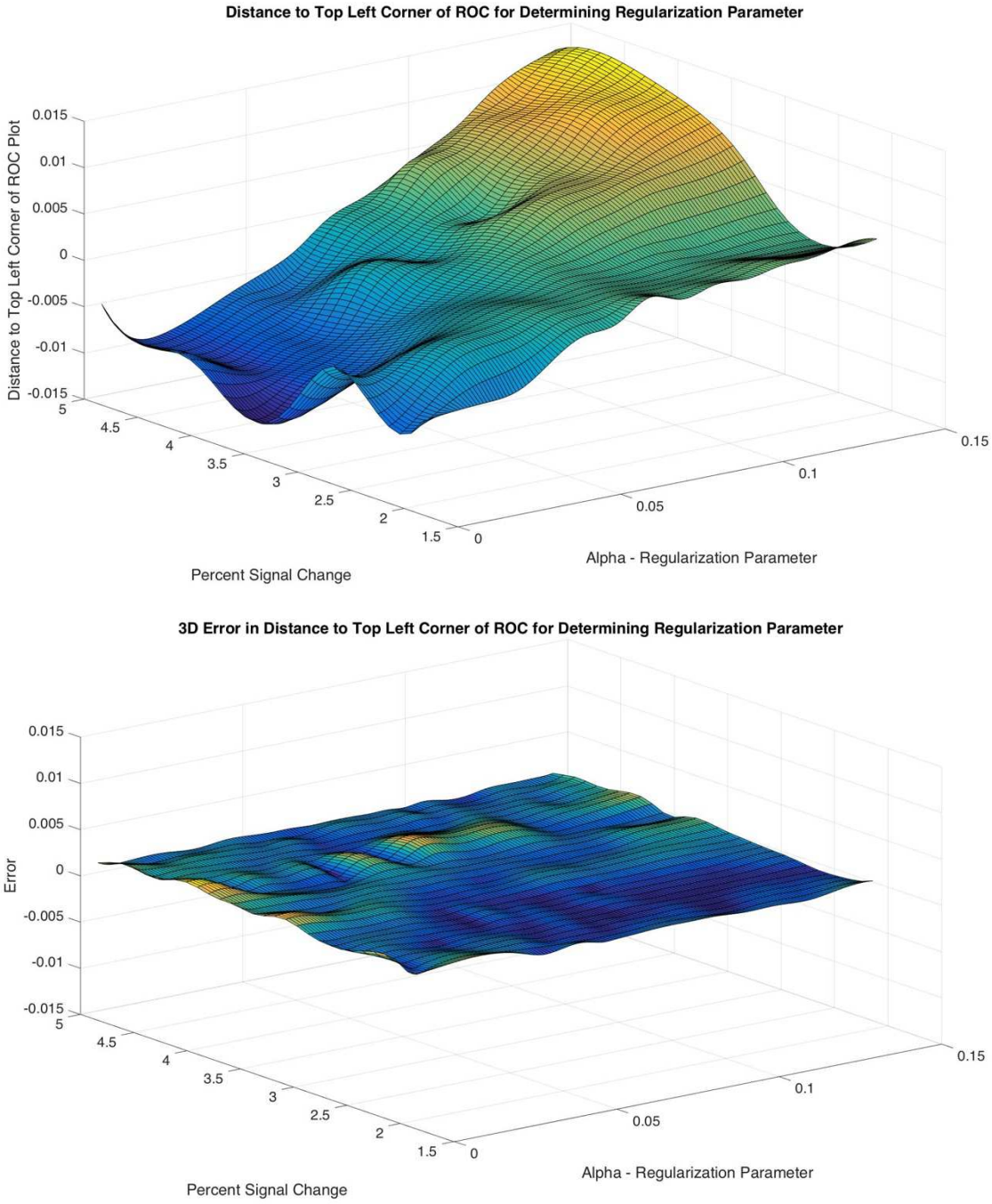

Figure 4.3 (Top) The vertical axis of this plot shows the distance to the top left corner of an ROC curve of spectral entropy in simulations. Low spectral entropy values were taken to be "active", and the optimal cutoff was chosen based on sensitivity and specificity. The results are plotted here as a function of regularization strength and percent signal change, and have been resampled to higher resolution using spline interpolation.
(Bottom) Error for the top plot, calculated using 5 sets of simulations with the same levels of activation and the same ROI. Low error compared to actual values gives confidence.

Variation of value of optimal sensitivity and specificity was expressed by standard deviation. This was arguably an optional parameter to consider since in general, it is the sensitivity and specificity that is most important in making regularized spectral entropy responsive to the amount of task-activation. The reason it was included, however, was to acknowledge that the response of spectral entropy with accompanying regularization should be consistent across datasets and even within a single scan where the amount of activation or signal strength will vary.

4.5 Effect of Regularization on Spectral Entropy

The goal of regularization was to improve the ability of spectral entropy to respond to signals that are rich in task information. This was done by increasing the sparsity of such power spectra in favor of the task frequency when appropriate, in a data-driven way. In turn, this sparsity reduced the entropy as seen in figure 4.4. This figure demonstrates the decrease in spectral entropy with increasingly powerful regularization on a single example time course.

The improved correspondence of spectral entropy with regularization to t-statistic is demonstrated in figure 4.5. Mentioned as part of the second hypothesis, these are used as proxy measures for the amount of task-related information contained in the fMRI signal.

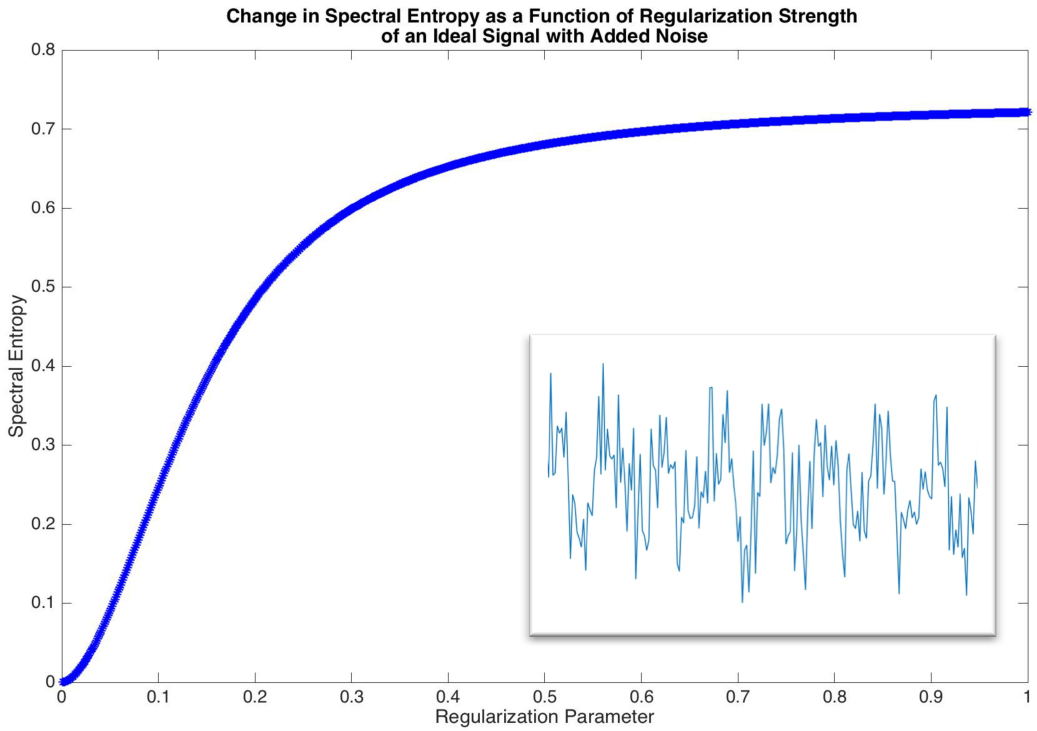

Figure 4.4 The spectral entropy of the signal (inset) is plotted with different regularization parameters. Lower parameters over-regularize the data and give spectral entropy that is too low, while high parameters have little effect, as seen in the levelling off of the plot.

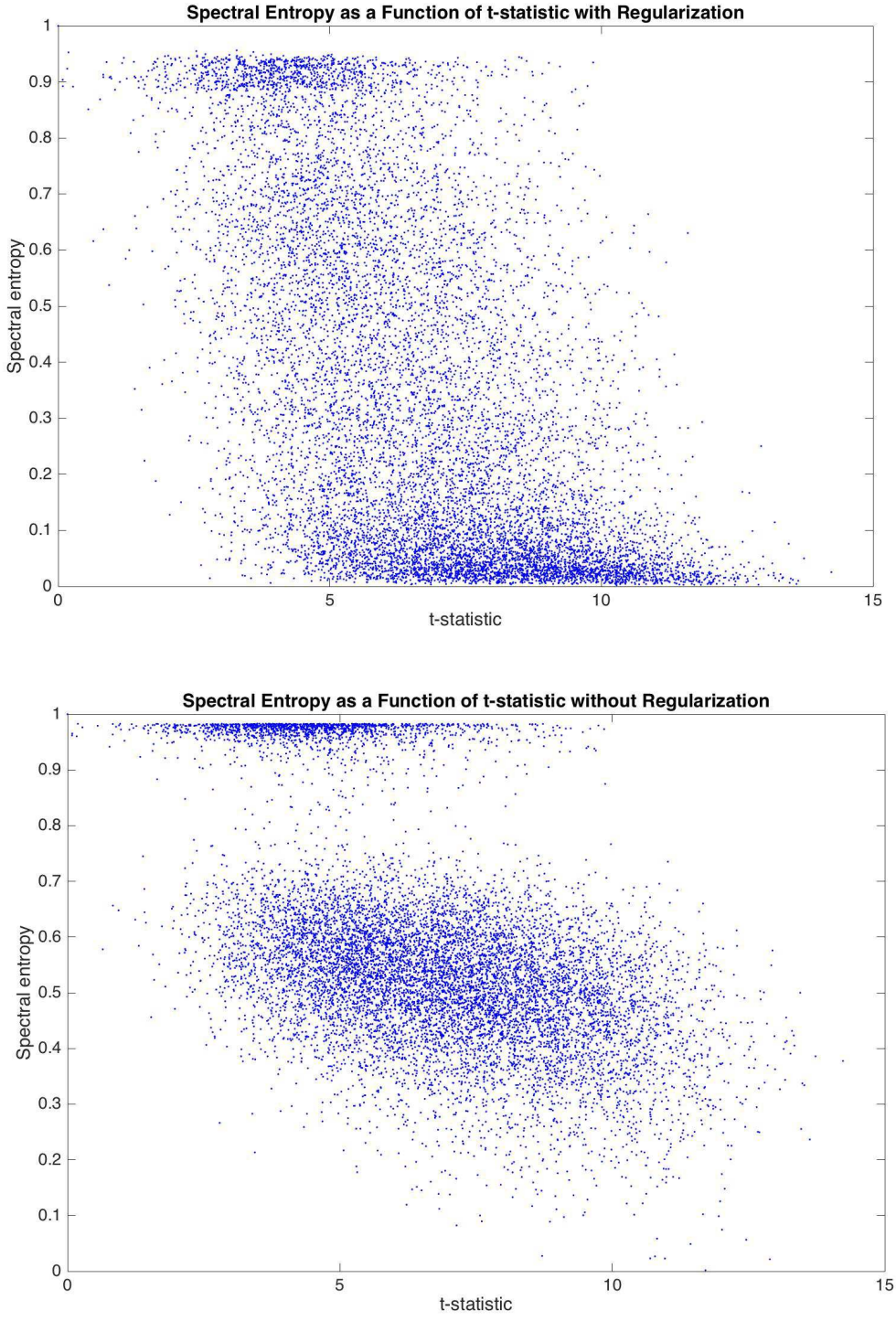

Figure 4.5 The change in spectral entropy relationship to t-statistic with (top) and without (bottom) regularization. Values were taken from the active ROI only of simulations with percent signal change between 2-5%. Addition of regularization dramatically reduces the spectral entropy values within the active ROI.

4.6 Justification for Regularization

The use of regularization was motivated primarily by the inevitable plethora of noise frequencies in fMRI data. Even an extremely clean scan with obvious functional activation will have a great number of frequencies present, and these frequencies will increase the spectral entropy. In the case of a signal that is dominated by the task frequency and is subjectively sparse to a viewer, these noise frequencies will make the signal appear objectively non-sparse to an algorithm such as spectral entropy. Increasing this sparsity, when appropriate, is the goal of regularization.

4.6.1 Challenges of Regularization

Regularization depends on some a priori knowledge of the data (in this case, the task frequency), and the challenge in regularization is determining how heavily to draw upon this a priori knowledge. If the regularization is too strong, the data is "over-regularized" and existing information overwhelms new information. In other words, the data becomes distorted such that it will only represent the a priori information and not the desired new information of the signal. In this work, this would be the equivalent of detecting a strong task-frequency in every single signal.

The need to balance regularization strength is an obvious disadvantage and challenge. It is a challenge because there is not a single obvious or correct way of determining regularization parameters. Having realistic simulations was fortuitous because it allowed calculation of sensitivity and specificity to optimize regularization. This was an elegant solution to balancing the issue of potential over-regularization, but is still not perfect. Because this method relies on the

simulations, it is only as good as the simulations themselves, and some sources of noise are hard to model or incorporate in simulated data. For example, motion artifacts were not included in the simulations.

Additionally, the choice of cost function to determine the regularization parameter will always be partly arbitrary. As discussed above in this work, the cost function included standard deviation and absolute distance to the top left corner of the ROC plot. This is justified by the need to optimize sensitivity and specificity (minimization of distance to top left corner of an ROC plot) and to give consistent results across difference effect sizes (minimization of standard deviation), but it is entirely possible that a better cost function exists.

Methodological issues are important to address, as well. Functional datasets use a lot of space in memory and are computationally intensive when in large numbers. To mitigate computational challenges, a limited number of percent signal change values were used to optimize the regularization parameter. Similarly, a limited number of α values were used. To compensate for this, spline interpolation increased the effective resolution of the 3D plot seen in figure 4.3. These 3D plots were visually compared with and without spline interpolation to ensure that the shapes were similar (i.e., that the interpolation did not over-interpolate surfaces that did not exist), but it is possible that more samples or finer interpolation could yield a more optimal α value.

Lastly, the determination of α using the method described here was repeated five times and error was calculated as also shown in figure 4.3. This gave confidence that the spline interpolation was not unrealistic and that the results were replicable.

4.6.2 Benefits of Regularization

The benefit of regularization was improved sensitivity and specificity of spectral entropy in identifying voxels rich in task-information. The core process behind this was increased distinction between low- and high-spectral entropy in active and inactive voxels. As seen in figure 4.6, a signal that is purely noise is not affected by the regularization in the same way that a signal dominated by the task is affected. This is due entirely to the data-driven nature of this regularization method and the fact that it's sensitive to the differences of frequencies in the power spectra, rather than the frequencies' actual power spectra values. Being data-driven is a built-in way to avoid some degree of over-regularization, and is a benefit of the method. Additionally, the use of sensitivity and specificity in simulations effectively avoided over-regularization by taking into account false positive findings.

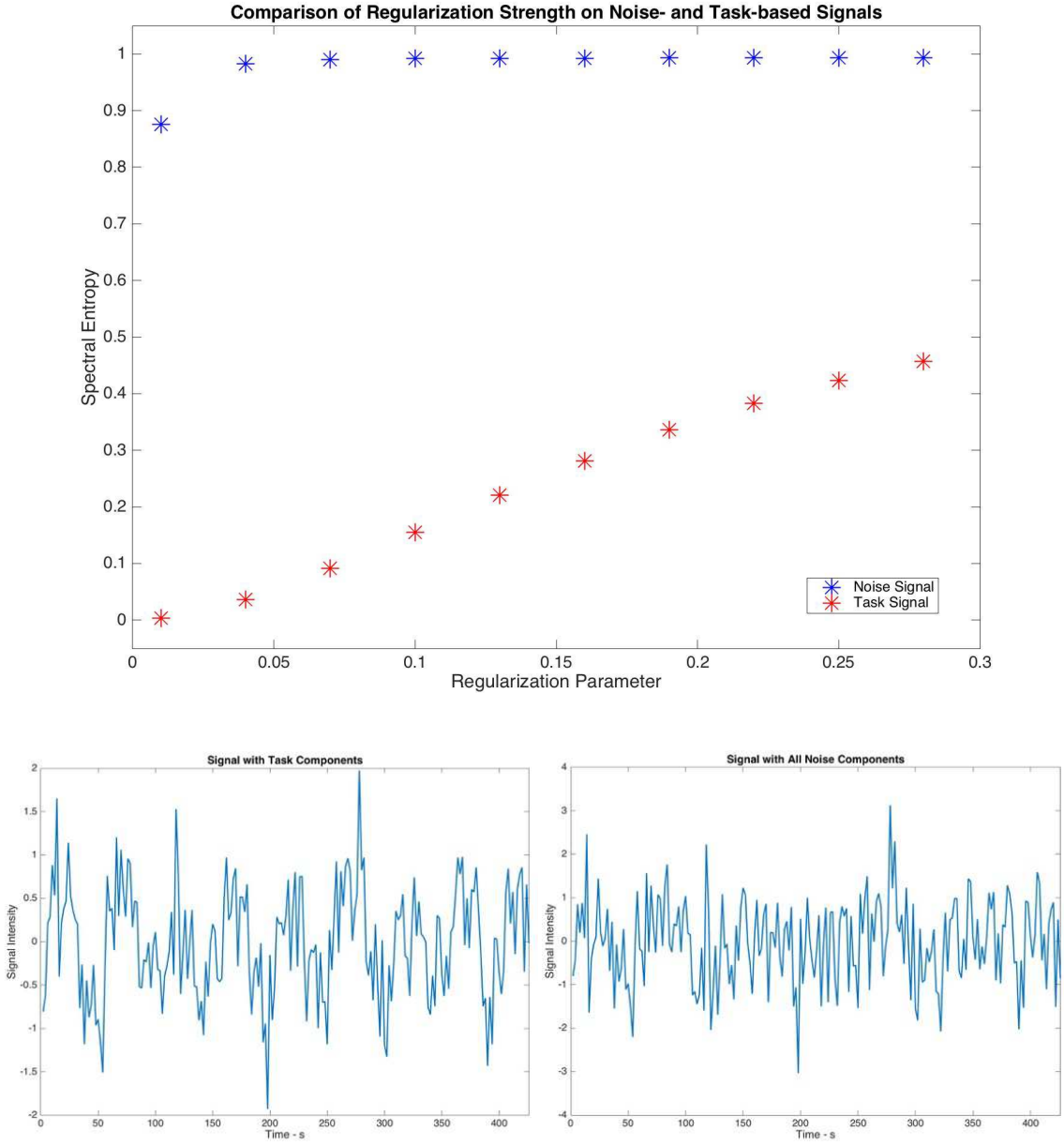

Figure 4.6 (top) Spectral entropy changes much more dramatically with regularization strength for a signal containing task information than a signal that is purely noise. The noisy signal's spectral entropy is relatively invariant, which is desired, but the task signal changes considerably. This demonstrates the data-driven nature of the regularization method. (bottom) The task signal is shown on the left, and the noisy signal on the right.

4.7 Conclusions on the Effect of Data Regularization on Spectral Entropy

Use of regularization in this work was motivated by the hypothesis that data-driven regularization would improve the ability of spectral entropy to detect useful task-related information. This was evaluated using the change in spectral entropy with regularization strength on a signal that was known to contain task-information, as well as by comparing the change in relationship of spectral entropy to t-statistic in the region of added activation of simulated data sets.

Spectral entropy was shown to decrease with increased regularization strength for signals that contained task information, but was shown to be relatively insensitive to those that were purely noise. This increased spectral entropy differentiation of these two signal types indicates that the hypothesis was satisfied and that the data-driven regularization does improve the ability to detect useful task-related information. Additionally, the relationship of spectral entropy to t-statistic in a known region of activation changed when data-driven regularization was added. Values of spectral entropy decreased, particularly those with higher t-statistic, in the regularized data compared to the non-regularized. This also confirms the hypothesis of the effect of data-driven regularization on spectral entropy.

Chapter 5: Comparison of Regularized Spectral Entropy to Other Methods of Quantitatively Measuring fMRI Data

The second, and most important, hypothesis of this work is that spectral entropy, especially when regularized, can measure information content related to task activation in fMRI signals. It was necessary to satisfy the first hypothesis, about data-driven regularization, before addressing the second hypothesis. This is because regularization is employed in the objective measures of the second hypothesis. In other words, to appreciate how the hypothesis of spectral entropy identifying useful information in task-based fMRI is fulfilled, it was important to discuss the role of regularization in working in concert with spectral entropy.

Spectral entropy was chosen for this work because of its ability to quantify information content in the frequency domain. The objective measures to test the ability of spectral entropy with regularization to detect useful information in fMRI signals were chosen because of their well-understood relationships to fMRI data. A scan that is too noisy will not be rich in task-based information and will also likely not produce a clean map with t-statistics high enough to be useful, for instance. Similarly, this additional noise will reduce the SNR of the signal. For these reasons, it was expected that regularized spectral entropy will correlate to factors such as SNR, T-statistic, and the amount of added signal in simulations.

5.1 Results

The following sections discuss objective measures that were used to evaluate the second hypothesis of this work surrounding regularized spectral entropy's correlation to other known measures of fMRI information content. These include t-statistic, percent signal change in simulations, and signal to noise ratio.

5.1.1 Correspondence to T-statistic

A higher t-statistic indicates better fit to an ideal voxel response to the task, and therefore higher likelihood that the voxel in question contains neurons that are active in response to the task/stimulus. This would also indicate that a voxel that is task-information rich should therefore have a high t-statistic and a low spectral entropy value (especially when regularized), as hypothesized earlier.

5.1.1.1 Simulations

Comparison to t-statistic is fairly straightforward because as every voxel has an associated entropy value, every voxel will have a t-statistic. The challenge is in data representation because of the more than 100,000 voxels in the 3D MRI image of the brain, only a small subset are really useful. To simplify and reduce the large number of potential data points, simulations were used; since the area of added activation is known, it's useful to only use data from this region. The range of activation strengths (percent signal changes) resulted in a range of different t-statistic values, all within the same ROI. These were extracted and compared to regularized spectral entropy values in figure 5.1.

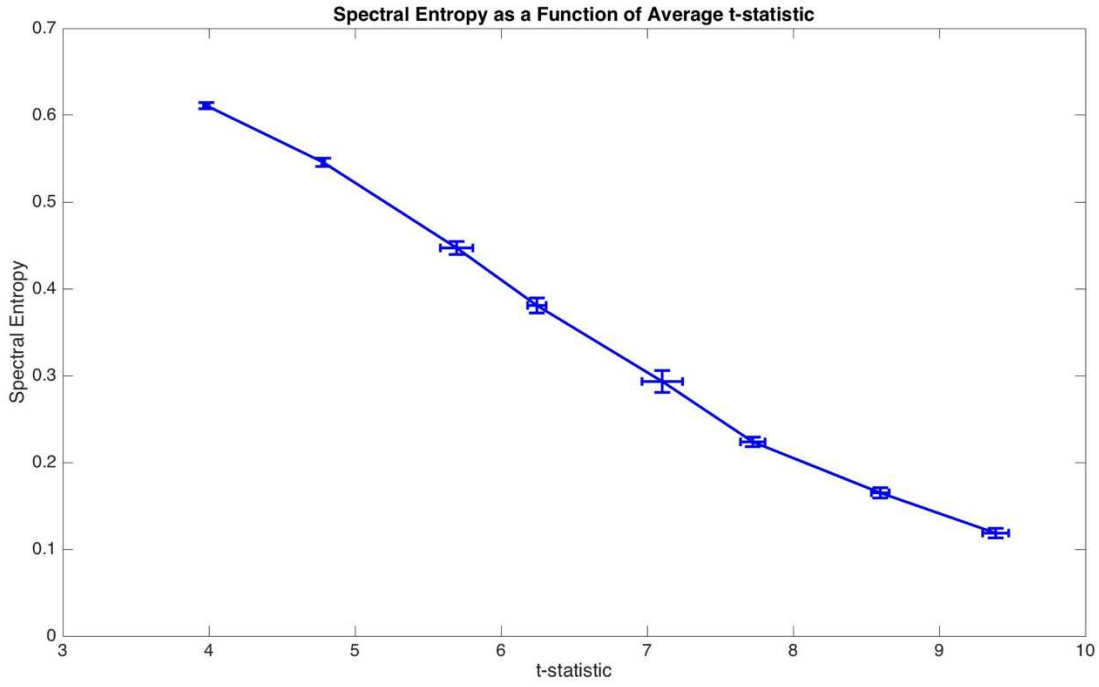

Figure 5.1 Regularized Spectral entropy decreases with increasing t-statistic in the active ROI of simulations of varying percent signal change.

Additionally, the relative sensitivity and specificity of t-statistic and regularized spectral entropy are compared later in figure 5.9. Unlike in real fMRI data where it is essentially impossible to know absolute ground truth (i.e., where there is truly activation that is task/stimulus related), simulations very conveniently offer the ability to construct true ROC curves. In the interest of best representing the sensitivity and specificity of each circumstance, the cut-off values for regularized spectral entropy and t-statistic that were chosen were simply those that maximized sensitivity and specificity.

Spectral entropy, even with regularization, is not quite as powerful as t-statistic in determining the region of activation, particularly for lower percent signal change around 2% (this is discussed later in more detail). However, regularized spectral entropy also requires less a priori knowledge and simpler

modelling. For example, there is no assumption regarding the shape of the haemodynamic response in regularized spectral entropy.

5.1.1.2 Real Data

Comparison to t-statistic in real data is more difficult because of the question, what voxels should be compared? The most straightforward answer is to include all voxels after applying as good a mask as possible to remove unnecessary signals from ventricles and outside the brain itself.

However, regularized spectral entropy maps of real data show activation in areas that did not overlap with t-statistic, such as the occipital lobe. There is clearly less than perfect agreement between the two modalities that is increased in real data compared to simulations. This is partially compensated for by using an absolute value of t-statistic, or as in figure 5.2 below, including voxels with negative t-statistic for comparison (these are ordinarily ignored in fMRI interpretation). Because of the large number of voxels, most of which do not have low entropy or high t-stat, histograms of low and high regularized spectral entropy vs. t-stat were made instead. By dividing the data into low and high regularized spectral entropy, it is more presentable and easier to interpret.

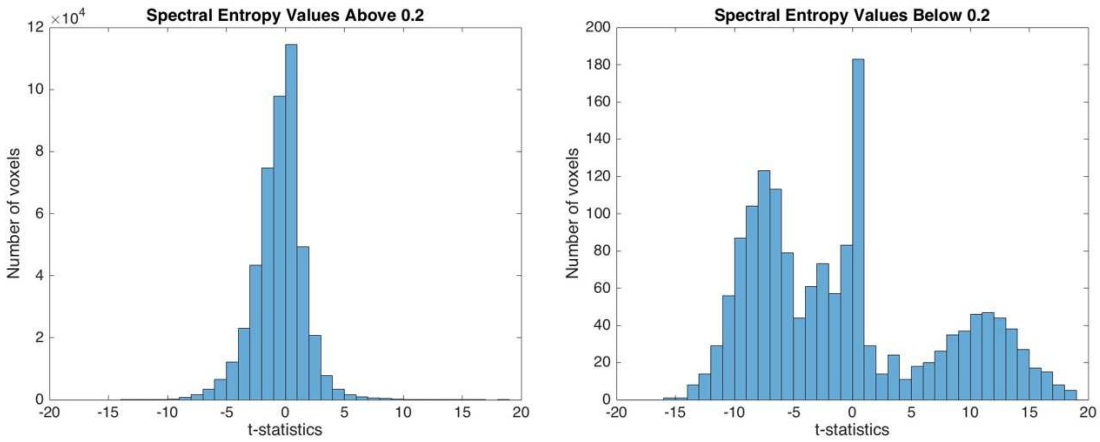

Figure 5.2 Voxels are grouped into two t-statistic histograms based on regularized spectral entropy values. High spectral entropy is shown on the left, and low spectral entropy is shown on the right. Low spectral entropy favors more extreme values of t-statistic, indicating a relationship to the amount of task-related information content.

5.1.2 Correspondence to Percent Signal Change in Simulations

The benefit for simulations is precise knowledge of the ROI of activation as well as how much activation is present. This is ideal to study the effect of added activation. Increased percent signal change means that there must be increased task information in the signal relative to noise, and increased sparsity in the frequency domain. It's a very reasonable assumption that greater relative activation in the form of percent signal change would ultimately mean lower spectral entropy. In figure 5.3, regularized spectral entropy is plotted as a function of percent signal change. The average regularized spectral entropy in the ROI has been taken from each scan (values outside this ROI have no percent signal change in all scans).

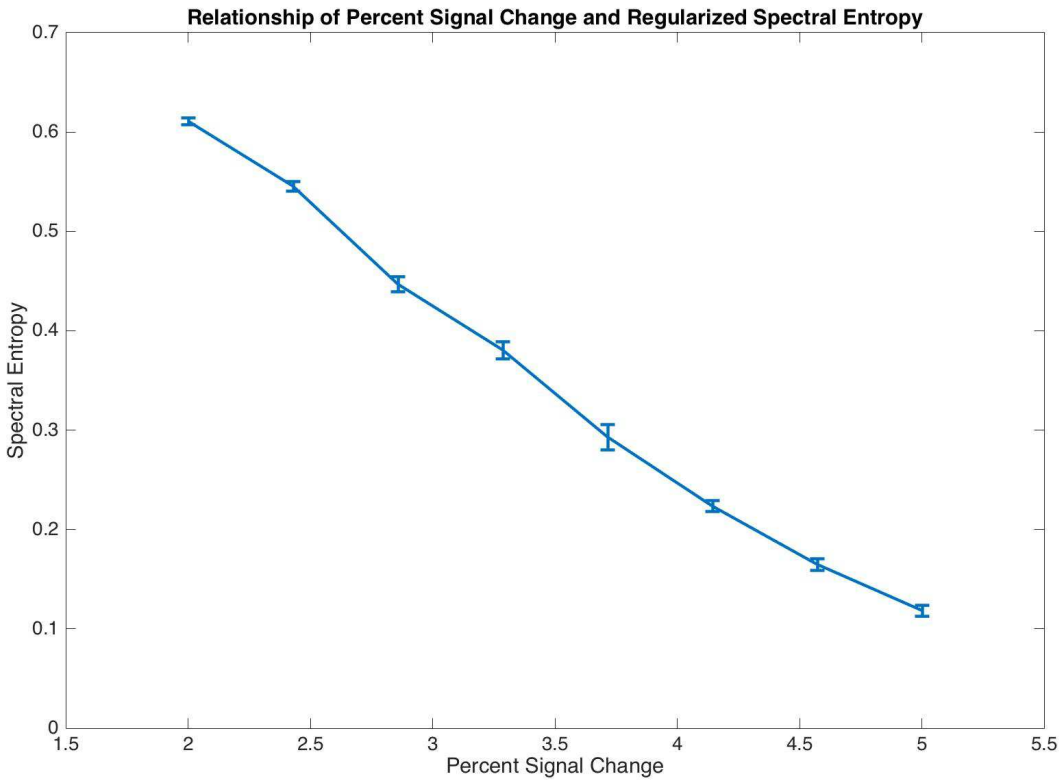

Figure 5.3 Regularized spectral entropy is seen to decrease with increasing percent signal change.

5.1.3 Correspondence to SNR in Ideal Functions

One of the first experiments in this work was the evaluation of how SNR effects spectral entropy. The reasoning is that additional noise (i.e. for an active voxel with low SNR) will result in difficulty of interpretation and may obscure the signal components resulting from the task. This noise will also increase the number of non-task frequencies in the signals' power spectra and decrease frequency sparsity while increasing spectral entropy. To test this, an ideal function had noise added to it and the SNR and spectral entropy were calculated. This is shown for regularized spectral entropy in figure 5.4.

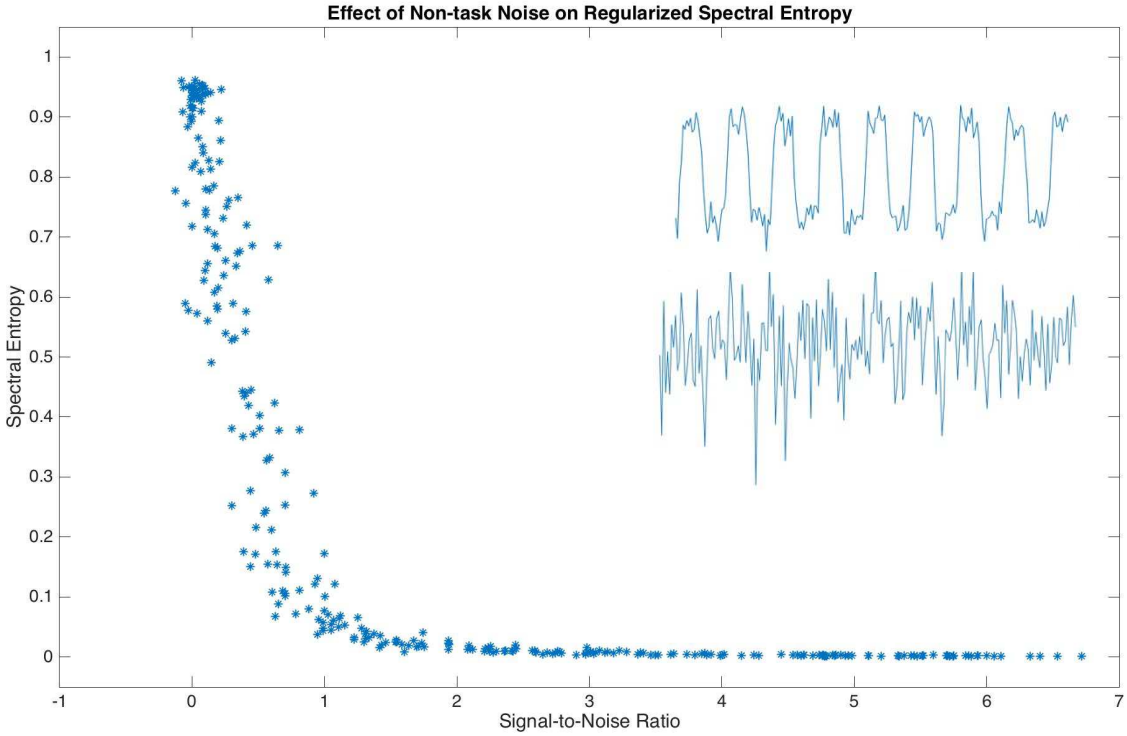

Figure 5.4 Added noise, measured through SNR, is shown to have a strong effect on spectral entropy. In this case, regularized spectral entropy is shown, but the phenomenon is similar, although weaker, for spectral entropy without regularization. Inset are examples of a high SNR signal (top) and low SNR signal (bottom)

5.1.4 Characterizing the Distributions of Entropy

A secondary hypothesis of this work was that regularized spectral entropy would produce meaningful spatial distributions. "Meaningful spatial distribution" indicates that regions of low entropy would correspond to known areas of activation in real data. In real data, there is no way to truly know where activation occurs, although knowing the task performed in the MRI does give some indication of what regions would be expected to activate. Since parametric models are the most common means of task-based fMRI processing and therefore have been more rigorously used than any other method, they are treated as a

"gold standard" here. The following figure is an example of language map processed using the GLM, and regularized spectral entropy.

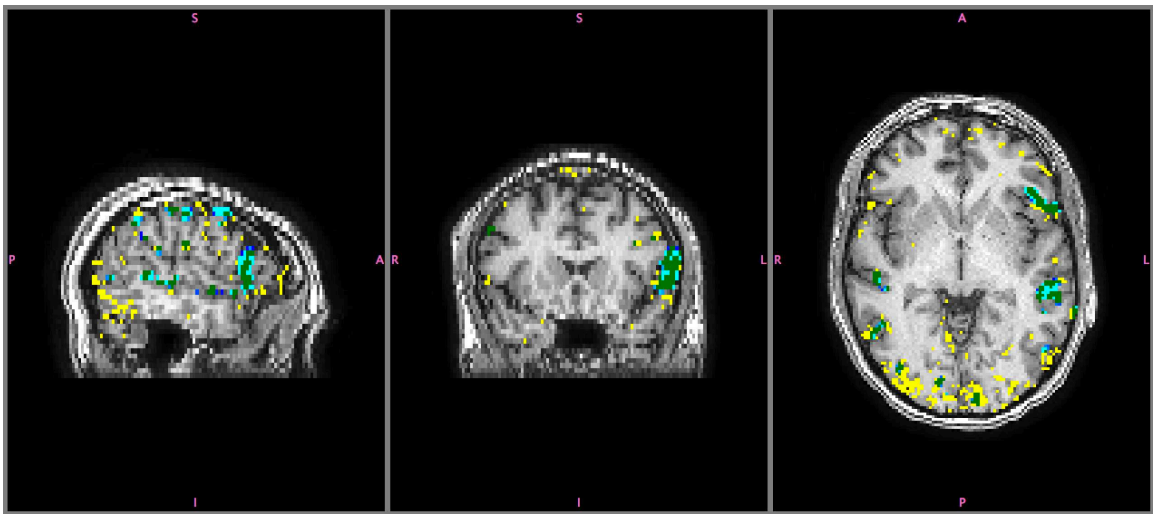

Figure 5.5 An example of an fMRI language scan. Regions in yellow have low regularized spectral entropy (below 0.2), regions in blue have high t-statistic (above 7) found using the GLM, and regions in green are overlap of low regularized spectral entropy and high t-statistic. Some low spectral entropy regions are seen around the occipital lobe that do not coincide with high t-statistic. It is possible that these regions are responding to the language task but are effectively removed through the contrast of the parametric model in the GLM.

Additionally, it was stated that distributions would have a consistent pattern that is replicable between subjects, especially if the subjects were performing the same scan. An average of 4 histograms of regularized spectral entropy distributions is shown in figure 5.6.

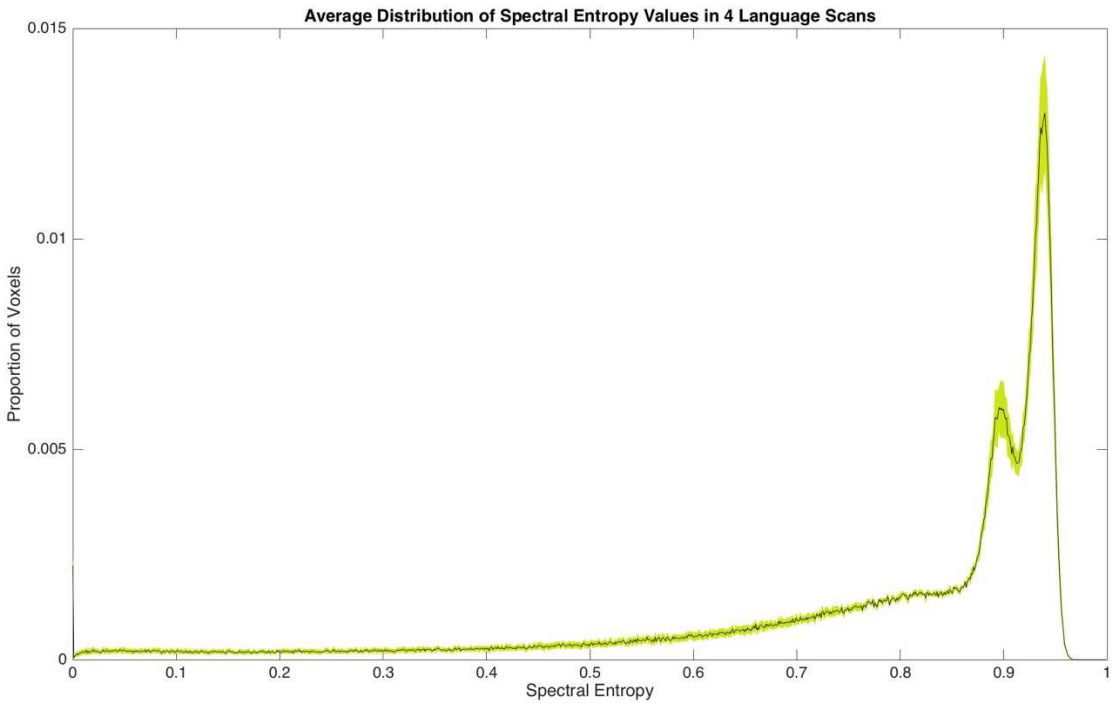

Figure 5.6 The average regularized spectral entropy distributions of four language scans. Regularization changes the shape of distribution slightly, but not the similarity between difference subjects' scans. Error between values is shown in yellow, and the average value in the dark line. This demonstrations consistency of spectral entropy distributions, and replicability between subjects.

5.1.5 Comparison of Regularized Spectral Entropy to Sample Entropy

Another method of validation of regularized spectral entropy was comparison of results to other published entropy measures in functional neuroimaging, especially those that map or identify areas of activation. The work of Wang et al., using sample entropy, is arguably the most similar to this application of spectral entropy in that maps of functional activation were also produced. In the case of sample entropy, the maps were made to demonstrate the effect of a task on the entropy of the brain. These maps were actually t-statistic

maps based on group-differences of voxel entropy values, and in this sense are quite different than spectral entropy maps.

That said, both forms of entropy are measures of information content in fMRI signals and information content that relates specifically to a task is particularly valuable. Regularized spectral entropy was shown to be particularly effective at finding information content specific to a task, and can make an interpretable non-parametric activation map on a single subject in less time that a typical parametric map.

The resulting activation maps are shown in figure 5.8. One major advantage of regularized spectral entropy is that reasonable maps can be produced from just a single scan, or that useful information relating to the presence of task-data can be identified in only a single subject. Since a range of datasets with varying percent signal change were used to calculate sample entropy maps but only single datasets are needed for both traditional GLM parametric maps and regularized spectral entropy maps, three representative maps from simulated data sets with 2%, 3.7%, and 5% were chosen to compare to sample entropy.

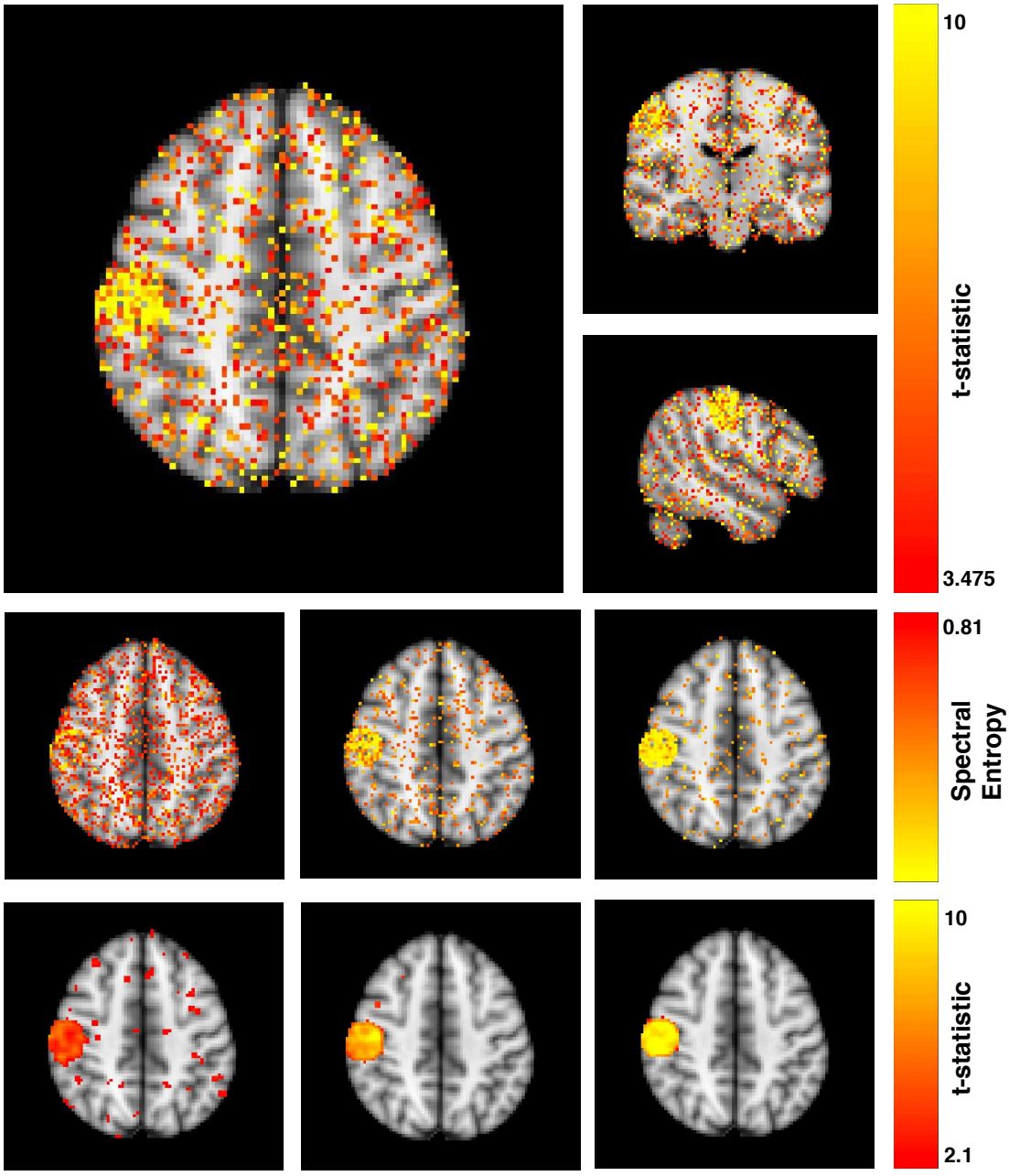

Figure 5.7 (top row) Axial, sagittal, and coronal views of a t-statistic map of the reduction in sample entropy from task to rest in 32 simulated data sets. (middle row) Regularized entropy maps for three example simulations of percent signal change 2%, 3.7% and 5%. (bottom row) Parametric maps of the same datasets as spectral entropy showing the "gold standard" in identification of task-active regions.

Additionally, the relative specificity and sensitivity of each method was calculated. This is shown in figure 5.9. For sample entropy, there is only a single value as all 32 data sets were required for the calculation of t-statistic showing the reducing in sample entropy. For the traditional GLM and regularized spectral entropy, specificity and sensitivity can be calculated for each effect size with error bars. This serves as a useful comparison of regularized spectral entropy to both the GLM and sample entropy. For comparison, the sensitivity of sample entropy was 0.7296 +/- 0.0086, and the specificity was 0.7532 +/- 0.005. These values are comparable to the sensitivity and specificity of regularized spectral entropy with percent signal change between 2-3%.

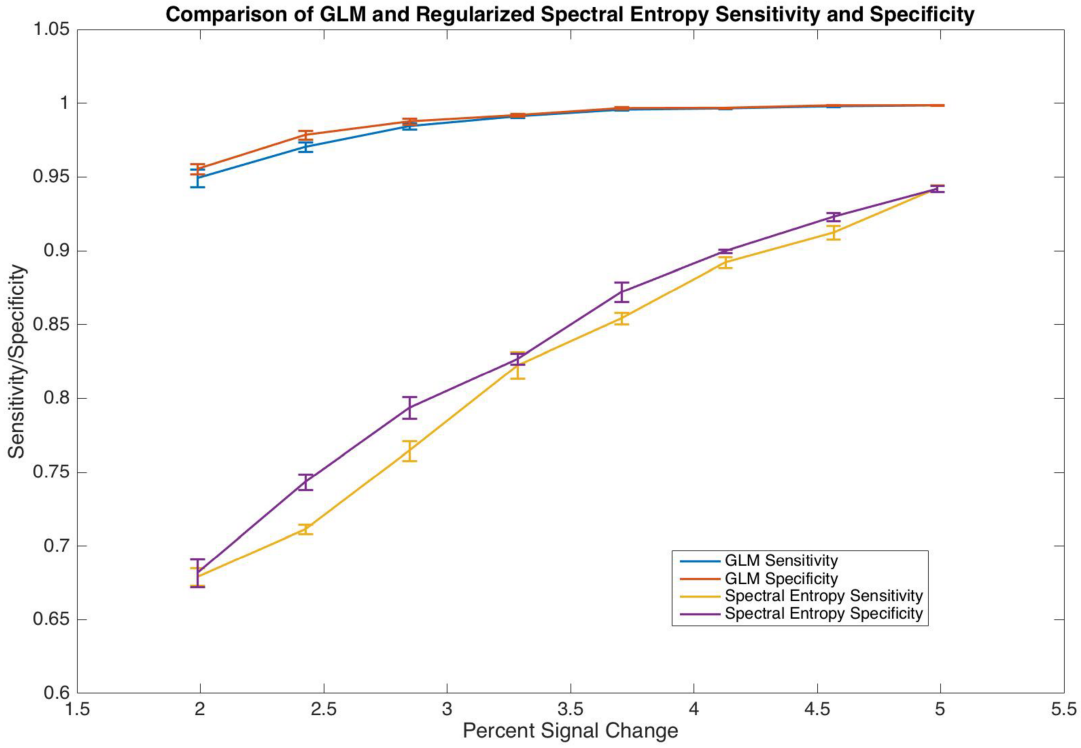

Figure 5.8 Changing sensitivity and specificity of parametric maps (GLM) and regularized spectral entropy. Error bars are from 5 replications of each simulated data set. Sample Entropy had sensitivity of 0.7296 +/- 0.0086, and specificity of 0.7532 +/- 0.005 for 32 simulations of varying percent signal change.

5.3 Discussion

A significant challenge in this work was identifying ways to relate regularized spectral entropy to known amounts of information content. In fMRI, the true areas of activation are not known, and the BOLD signal is itself a secondary measure of activation. Similarly, even when there is confidence that a particular region is active, it's not necessarily clear how much of the signal is noise. To accommodate this, a number of different proxy measures were used to develop, test, and validate regularized spectral entropy.

5.3.1 Comparison to T-statistic

The first quantity compared was t-statistic and the reasoning for its use was two-fold. First, it is an extremely common activation measure in research and clinical use. As such, most people familiar with fMRI have an appreciation and understanding of the role of t-statistic, what it represents, and its strengths and limitations. In general, t-statistic is accepted as a measure of identification of areas of activation.

Secondly, t-statistic can be thought of as an indirect measure of the amount of useful information content that relates to a task in a voxel. The higher the t-statistic, the greater the likelihood that components of that signal are due to task activation. For example, voxels with low t-statistic would be ignored in fMRI analysis and assumed to have little relation to the task. Similarly, someone interpreting a parametric map would have much more confidence that a voxel with a high t-statistic contained desired information.

There are some issues with comparing t-statistic to regularized spectral entropy, however. Spectral entropy is invariant to phase, while t-statistic is very

dependent on phase. It is not an uncommon process for some clinical centres to shift their parametric model temporally to best match up to the haemodynamic latency of patients, for example, thereby increasing statistical power and ability of the parametric model to identify activated regions.

Spectral entropy (regardless of regularization) also does not depend on the latency of the response: some regions of the brain or individual subjects may have a faster or slower change in CBV and this will influence the t-statistic computed in the GLM. If the latency of response is large, the phase of the ideal task will be significantly different than that of the actual response and the correspondence will not be great in the parametric model. Spectral entropy, however, is resistant to phase changes in that it does not respond to them. Potentially, the non-response of spectral entropy to phase may have (as of now, currently unevaluated) applications in analyzing latency of response due to task conditions, individual latency differences, and spatial changes in latency.

Both haemodynamic inhibition and suppression effects are huge and important topics that cannot be given the attention they warrant in this work. They are briefly discussed here, however, because of their interaction with spectral entropy. Known inhibitory haemodynamic processes in the brain, as well as the often-complex role of contrast in fMRI studies, voxels with frequencies that match the task-frequency but not the phase are likely still in some way reflecting execution of the task (Henson et al., 2003; Liddle, Kiehl, and Smith, 2001). For example, some regions may be unintentionally activated by the contrast but not the task. This might result in a negative t-statistic value, which is generally disregarded in fMRI interpretation, and is not ideal (in a perfect situation, the contrast activates undesired regions as much as the actual task).

However, this response to a contrast still indicates that the subject is responding to the fMRI stimulus and that, most likely, useful information is being acquired.

Similarly, it is well reported that certain parts of the brain experience haemodynamic suppression in response to other regions' activation (Friston, Mechelli, Turner, and Price, 2000). This would, again, either be detected as a negative t-statistic or very low t-statistic, but is still indicative that the task is being processed in the brain and from the perspective of this work is therefore considered useful task-related information.

For real data, some of the disagreement between values, such as low regularized spectral entropy and low t-statistic, can be attributed to low frequencies ineffectively removed by the regularization. Part of the preprocessing for the calculations in this work involved removal of all frequencies below the task-frequency. Voxels are the edge of the brain are often most affected by motion, however, and task-related motion will have the same frequency of the task. The effects of this temporal change to the signal are impossible to completely remove, even rigid body motion correction, without complex correction methods. This may explain some of the low entropy values seen near the periphery of the brain in real data. It's important to note that task-related motion is still task-related information, and so if this is the case, regularized spectral entropy is still identifying signals concerning the task. In other words, if motion is due to the task, there is reason to believe that the subject in the MRI is in some way responding to the task stimulus. However, the effects of task-related motion may still degrade data, and so effective means of detection and correction for this motion would will always still be necessary.

5.3.2 Comparison to Percent Signal Change

These reasons for disagreement or challenges in the use of t-statistic as a means of measuring the ability of regularized spectral entropy to detect useful task-based information were one reason for employing other measures, such as percent signal change in simulations. In fact, simulations were critical to this work for the ability to control a known area of activation and degree of activation. Presumably other ways of measuring the degree of activation could be used, but percent signal change was chosen for ease of comparison to known values in the literature.

A critical assumption is that greater percent signal change due to a task is directly related to the amount of task-related information contained in the signal. In a simulation, all voxels will have a comparable amount of noise added (physiological, white noise, autocorrelation, etc.). In the absence of added activation, a given voxel is effectively composed of 100% noise and 0% activation. As the percent signal change increases, these proportions change in favor of activation. Thus, the percent signal change should be directly related to the amount of desired task-based information in the signal.

There are still some problems with using fMRI simulations, despite the extreme convenience of being able to change the amount of added activation. We were careful to modulate noise parameters such that they were realistic, but the "cleanliness" of maps made based on simulations is still unrealistic, and this suggests that simulations cannot truly account for all of the variability in real data sets. Some factors that simulations are not effective at incorporating are motion, partial volume effects, and signal loss due to regional depth within the brain. Another minor problem that could be mitigated is the "drop-off" of signal

at the edge of activated ROI's: in reality, signal does not sharply end but fades off. It would be possible to simulate motion in fMRI, but it is unclear if simulated effects can be as pervasive as the dramatic signal spikes from motion that typically are so damaging to fMRI signals.

In general, the knowledge of ground truth was sufficient to warrant using simulated data in this work. Varying percent signal change within normal parameters replaced the need for signal drop-off at the edge of active ROI's as variations in signal strength were therefore accounted for through multiple data sets. More importantly, the need to rely on secondary measures of information content such as t-stat was reduced by being able to more directly adjust the amount of task-based signal present.

5.3.3 Comparison to SNR

Comparison of SNR with regularized spectral entropy was similar to the comparison with percent signal change in that signal to noise ratio can be assumed to represent the amount of useful task-related information compared to noise in the signal. In this particular case, this assumption was directly built into the analysis method. Two signals were created: one was random noise, the other an ideal voxel's response to the task. The SNR was varied by adding the noise to the ideal response in varied amount, and then calculated using MATLAB's snr function ("snr Documentation", 2017). Clearly, when the signal is 100% noise, the SNR is very poor. When it was 100% signal, the SNR is extremely high.

This also relates directly to information content relating to the task. When there is no added noise, the information content can be completely attributed to the task. This represents a case where the spectral entropy should be very low,

reflecting the sparsity in the frequency domain. In the case of significant added noise and low SNR, spectral entropy will be very high and will reflect a lack of sparsity in the frequency domain. In other words, the many sources of noise contribute many different frequencies that appear in the power spectra.

5.3.4 Characterizing Distributions of Regularized Spectral Entropy

Similar to distributions of sample entropy (from the Brain Entropy Toolbox), there is a replicable distribution of spectral entropy. The implications of this are that there might be a typical entropy value for certain non-neocortical regions. The exact value of entropy will change depending on if it is regularized and what regularization parameters are used, but will remain similar across subjects provided the choice of regularization and other parameters remain constant. Perhaps white matter or grey matter not activated by the task have consistent and replicable levels of spectral entropy that are reflective of normal biological function. The consistency of the spectral entropy distributions is promising, however, because it indicates replicability. This is further confirmed in the example spatial map shown, as well. From this map it was seen that areas of anticipated activation had low regularized spectral entropy, confirming that voxels responding to a task are in fact, sparse in the frequency domain and favor the task frequency.

5.3.5 Comparison to Sample entropy

It's important to discuss how the intention of the Brain Entropy toolbox (BENtbx) made by Wang et al. is different from that of this application of spectral entropy. The main focus of BENtbx is to map natural distributions of entropy in the brain, which were found to have unique associations with the neocortex.

Identifying functional activation in group studies was a secondary hypothesis and performed to show a special quality of regularized sample entropy, but not the primary aim or purpose.

To compare sample entropy and regularized spectral entropy, a replication of Wang et al.'s work was performed using simulated data. Wang et al. showed a decrease in sample entropy in areas of functional task activation in a group of 16 subjects who were scanned four times each: two scans were task-scans and two scans were resting state for each subject. BENtbx maps were produced for each scan, and the difference of resting state and task sample entropy maps were calculated. From these difference values, a t-statistic was calculated to produce the final map.

To replicate this fairly with simulated data, reasonable levels of activation ranging between 2-5% percent signal change were used to make 32 maps. Eight values of percent signal change were used, so that there were four examples of each percent signal change value in the dataset. Instead of producing 32 resting state scans, which take not only require a lot of data storage space and also computation time to produce, a single resting state simulation was made with identical noise parameters to the task-based simulations. Knowing that the signal strength and noise parameters would be identical throughout the brain in a resting state simulation, with the exception of ventricular and extra-brain areas that are masked out, voxels were randomly sampled to compare to the task-scans. For each task-scan voxel with a given sample entropy value, the difference was calculated from the sample entropy value of a randomly chosen voxel in the resting state scan. Therefore for every voxel, 32 difference values existed in which to calculate a t-statistic.

Something to note is that the GLM performs better in terms of sensitivity and specificity, but that it also requires more assumptions and a priori knowledge, computation time, and pre-processing. Computation time is not directly addressed in this work because of differences in coding language and software packages. Regularized spectral entropy was coded in MATLAB in this work, and requires approximately 1 minute and 30 seconds to process an fMRI scan with 213 image volumes. An efficient parametric model pipeline can process the same data in 2-3 minutes.

5.3.6 Strengths and Weakness of Spectral Entropy

One of the weaknesses of spectral entropy – regularized or not - is that it responds specifically to frequencies, and it is not guaranteed that a signal with a strong task-frequency is actually due to the task. It is unlikely it's due to another source, especially given the range of most task frequencies compared to other frequencies. A task frequency will typically be approximately 0.02-0.03Hz. Low frequency drift, which is easily removed in pre-processing, will be lower than this. Noise frequencies will be higher, as well as physiological noise. Signal due to heart rate is typically around 1-2Hz (Biswal, Deyoe, and Hyde, 1996). One confounding source of task frequency may be task-related motion, however, which is very common (Kochiyama, 2005). Patients may lean their head to better see the screen performing the task, or move their heads in some response to the task. It's arguable if this constitutes useful task-based information: task-related motion indicates that the patient is responding to the task, but it also reduces the quality of the data.

The lack of sensitivity to phase is also a potential weakness of spectral entropy. Again, however, response to stimuli that is out of phase is still indicative of a desired task-response.

There are a number of strengths to application of spectral entropy to fMRI as well, especially when combined with a regularization method as in this work. Spectral entropy is non-parametric, so effects such as an assumed HRF are not relevant (regularization is minimally parametric here). Other assumptions associated with a parametric model, such as the latency of response to the stimuli, are similarly not a problem. An assumed HRF is a particular challenge in parametric modeling, and one that has been questioned in recent years. There is evidence that not only do different individuals have variable HRF's and neurovascular coupling, but different parts of the brain may also have different effects (Handwerker, Ollinger, and D'Esposito, 2004). This reduces the ability of a parametric model that assumes a constant HRF to detect activation.

Parametric models also inherently involve statistical thresholding, and the results depend on the choice of threshold. Determining if a scan is of useable quality or contains useful information based on such a threshold is problematic and someone intimately familiar with expected activation is required to make this judgement. For example, too low a threshold will produce far too much activation which will mostly be spurious. Conversely, a high threshold may result in areas of true activation being eliminated. Both cases could give the incorrect impression of poor data quality. Spectral entropy resolves this by being non-parametric, and with the addition of regularization, the entropy difference between active and inactive voxels is more exaggerated. The property of being non-parametric also allows generalizability: regularized spectral entropy only

requires knowledge of the task frequency, and knowing this frequency, can be applied to any block design fMRI scan.

The difference of regularized spectral entropy between active and inactive voxels can be seen in histogram distributions. The results of a subject who was not responsive to the task in one scan but was responsive in a subsequent scan is shown in 5.7:

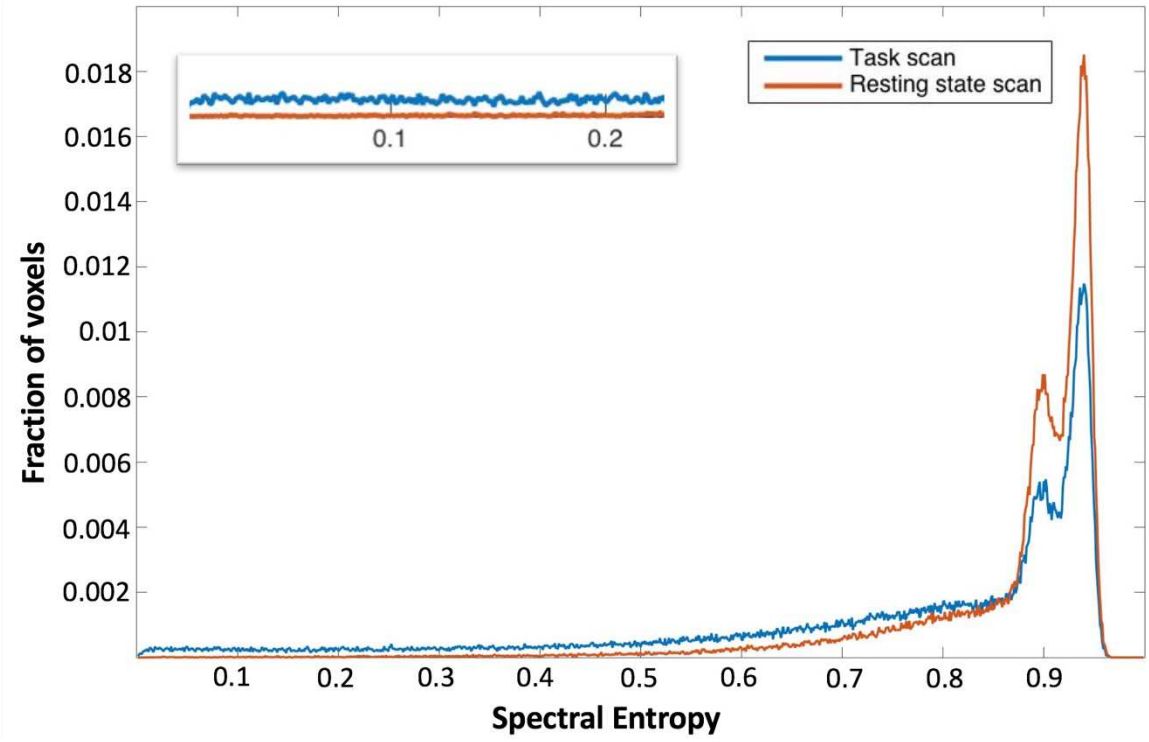

Figure 5.9 Difference in regularized spectral entropy distributions on the same subject when performing the task (blue) and resting (red). The inset shows the greater fraction of low spectral entropy voxels when the subject is actually performing the task.

In the low entropy end of this figure, the number of voxels is much higher for the case where this patient actually completed the task.

The replicability of regularized spectral entropy distributions is another strength of the method, and is in agreement with other measures of entropy in the brain (Wang et al., 2014). The similarity of distributions, shown in figure 5.6 earlier, indicates this method can be applied to different scans and the meaning

of the entropy distributions will be similar. The spectral entropy results are definitely not random or without meaning. It's important to note that these distributions are sensitive to the type and strength of regularization, and it's therefore important to always use the same regularization when combining the spectral entropy from different datasets. In the example shown in this work, regularization was included to be consistent with other figures and examples.

5.4 Conclusions on the Relationship of Regularized Spectral Entropy to Known Measures of fMRI Information Content

The second and main hypothesis of this work was based on the ability of regularized spectral entropy to detect useful task-related information content. This was addressed using objective measures of its relationship to SNR, t-statistic, and the percent signal change in simulated data sets. Relationships between regularized spectral entropy and these quantities were demonstrated, satisfying the hypothesis that spectral entropy would correlate to known factors of useful information content in fMRI signals.

The secondary hypothesis that meaningful maps of activation could be produced using spectral entropy was also satisfied, as well as that consistent distributions of regularized spectral entropy between subjects would be observed.

Chapter 6: Conclusion

While various examples of applications of information theoretical methods to fMRI exist, this work is the first known example of an application of regularized spectral entropy. It is also the first known example of an application of information theory to develop a potentially holistic and continuous measure of fMRI data quality. The use of regularization to increase the sensitivity and specificity of spectral entropy is particularly unique.

6.1 Future Directions

A potential use of regularized spectral entropy is as a holistic quality-assurance metric that works in real-time on scanners for fMRI protocols. To this end, many of the potential future directions of this work are motivated by this application.

6.1.1 Increases in Algorithm Efficiency

It was briefly discussed earlier, the scripts for this project were written almost entirely in MATLAB, while parametric mapping typically takes place in an optimized environment using a software package such as AFNI or FSL (Cox, 1996; Jenkinson et al., 2012). Even though regularized spectral entropy still produces results faster than the GLM, optimization could improve this further. Code optimization would likely most benefit from a more efficient coding language, such as C, rather than MATLAB. Methods of more quickly loading functional datasets (currently loaded as NIFTI files), possibly as DICOM files, would also speed up processing. These may be heavily dependent on the coding environment. Since fMRI processing packages are already designed to efficiently

load fMRI datasets, integration with the code of such a package may be an obvious first step.

Related to speed optimization of code is adapting regularized spectral entropy to process partial datasets, i.e. incomplete data sets that are growing during a scan. This would allow regularized spectral entropy to be used as a real-time source of information content in a scan, and therefore a potential quality control measure. The best way of doing this would likely involve an intelligent means of appending time series data on existing data to avoid reloading entire datasets repeatedly.

6.1.2 Improvements in Algorithm Performance

Improvement of the regularization methods and parameters may also be a worthwhile future investigation. Tikhonov regularization was found to be very effective at increasing the difference of spectral entropy between active and inactive voxels here, but some disagreement still existed. For example, the GLM still had better sensitivity and specificity in simulations. And in real maps, perfect overlap of GLM activation and low spectral entropy voxels was not observed.

It is possible that other forms of regularization could be more effective than the Tikhonov method employed here. This method was chosen because of its relative simplicity and ability to be data-driven, but other version of L1 or L2 regularization may be even more effective and could be explored.

Other adjustments to the regularized spectral entropy algorithm may also improve its performance. Currently, regularized spectral entropy does not take into account phase information, despite the fact that phase may contribute value

to the ability of spectral entropy to detect information-rich voxels. An early investigation of the role of phase had promising results in a small number of subjects. In this phase experiment, phase information was extracted from the Fourier transform data prior to calculation of power spectra. Regions of low regularized spectral entropy were isolated and used to create a mask. The phase values were then used to colour the voxels in this mask, and the results showed clusters of regions with similar phase that corresponded to known functional regions. For example, the data used was from a language scan and canonical language areas with low regularized spectral entropy in the left hemisphere had a distinctive phase from non-canonical language regions with low regularized spectral entropy, such as those in the occipital lobe.

Using cluster analysis (removing voxels of low spectral entropy that are not part of a cluster of a given size) may also be an effective way of improving the performance of this algorithm. This is based off a method of producing parametric maps sometimes used in fMRI (Forman et al., 1995). Early experiments with this method were not successful because of the scattered nature of some of the low spectral entropy voxels in real scans. When combined with improved regularization and other optimizations, however, clustering may be very effective and increasing sensitivity and specificity to activated voxels.

Continuing to think in terms of a real-time quality assurance metric that holistically evaluates the useful information content relative to other sources of information or noise, characterization of entropy distributions is likely the final major region of future work in regularized spectral entropy. It was found in a single subject that there is a difference in the number of low- and high-entropy voxels between task and rest data, and a very early experiment in this work prior

to the implementation of regularization found a difference of spectral entropy distributions in a small sample of task and rest data from the Human Connectome Project (HCP) (Van Essen et al., 2013). These differences were visually obvious but difficult to numerically quantify. Attempts to quantify the entropy distributions of scans included calculations of Kurtosis and Skew, but neither was found to be effective. The reason for this is suspected to be the very stretched shape of spectral entropy distributions: they do not really form a Gaussian curve.

Other attempts to quantify spectral entropy distributions included applying a mixture model. When observing a spectral entropy distribution, with or without regularization, two peaks clearly dominate in the high-entropy region. This suggests that a mixture model may fit the data well. If a model could be created based on a large number of scans, differences of an individual scan to this model may quantify the amount of task-rich information content present. Fitting a mixture model to these distributions never proved even remotely successful, however, perhaps an average of a great number of scans could be used to form a "template", like a regularized spectral entropy version of the MNI152 brain. This could be potentially used for information an AI classifier or other metric to identify data sets that have an acceptable degree of useful information content.

One last investigation that may be useful to continue is creation of a "bootstrap" spectral entropy distribution. A "bootstrap" fMRI dataset was created from a single time course extracted from a scan of the author's own brain performing a language task. The time course was taken from a voxel known to be responding to the task. This time course was resampled repeatedly and

randomly to create a new time course for each voxel in a template brain. In the first case, repetition of sample points was allowed (i.e., a given time course may have repeats of the same time point from the original signal). In the second case, no repeats were allowed so that every time point in the original signal was used, in a different order each time. The goal of this is to create a "standard entropy distribution" with particular regularization parameters, one that would be expected from purely random signals that may or may not contain any trace of task and could therefore be compared to real distributions to qualify the amount of task information present.

6.1.3 Potential Algorithm Outputs

If this work proves to be useful as a component of a quality-assurance tool for real-time fMRI scanning, it is worthwhile to hypothesize some potential outputs that would be interpreted by the individuals performing the scan. Currently, a "red-yellow-green" colour warning is used on some scanners to describe motion parameters. If a similar system is applied based on regularized spectral entropy, it would first be necessary to quantify distributions of regularized spectral entropy and relate these distributions to a "standard" distribution."

Such a standard distribution may come from any of the potential characterizations described above, such as comparison to a "boot-strap" brain. A normalized numerical value quantifying the relative proportion of low-entropy voxels compared to a that of a "boot-strap" brain may be used, for example. Similarly, while Kurtosis and Skew were unsuccessful experiments, a different measure may be employed and converted to a useful measure.

6.2 Summary Conclusions

This work was motivated by the broad goal of developing a metric that holistically represents fMRI data quality in real-time. It was not intended to solve this problem on its own, but is part of a larger body of work that will continue to move towards this goal.

Spectral entropy was chosen as a method of quantifying information content because it is calculated in the frequency domain, and frequencies are a critical part of the fMRI signal as they relate directly to task response, noise, and artifacts such as magnetic field drift. Much of this work was based around testing and tuning the ability of both the regularization and spectral entropy calculation to respond to task-based information. Regularization was introduced as a way to counteract unavoidable noise in fMRI signals and increase the sensitivity of spectral entropy to signals dominated by the task frequency. Regularization parameters were adjusted using simulations where the degree of activation (percent signal change) and location of activation was precisely known.

Regularization was found to effectively increase the sensitivity and specificity of spectral entropy to identify voxels that were rich in information content. Having demonstrated the usefulness of regularization as well as the consistency of distributions, comparisons to other measures relating to task-information content were performed. Regularized spectral entropy was found to correspond to t-statistic in the GLM, SNR in an idealized signal, and also to percent signal change. Because none of these measures are a direct quantification of the amount of task-based information content present in a signal (although percent signal change and SNR come close), all three measures were used to validate spectral entropy as exhibiting a correlation to data quality.

Regularized spectral entropy was also found to perform as well or better than sample entropy (found using the BENtbx). Perfect comparison wasn't possible because of the nature of calculation methods, but with single datasets that had percent signal change of between 2-3%, regularized spectral entropy was found to have sensitivity and specificity comparable to sample entropy calculated from a collection of 32 datasets with percent signal change varying between 2-5%. The sensitivity and specificity of spectral entropy was less than that of a traditional GLM parametric map, but also required significantly less a priori information and calculation time.

The ability of regularized spectral entropy to respond to useful task-related information content in fMRI signals, as well as its consistency between scans, suggests that it is a promising step in developing a holistic quality metric for fMRI data. Ultimately, it is hoped that this may function as part of a real-time system on MRI scanners to aid in data collection.

References

Alpert, G. F., Hein, G., Tsai, N., Naumer, M. J., & Knight, R. T. (2008). Temporal characteristics of audiovisual information processing. *Journal of neuroscience*, 28(20), 5344-5349.

Alpert, G. F., Sun, F. T., Handwerker, D., D'Esposito, M., & Knight, R. T. (2007). Spatio-temporal information analysis of event-related BOLD responses. *Neuroimage*, 34(4), 1545-1561.

Attwell, D., Buchan, A. M., Charpak, S., Lauritzen, M., MacVicar, B. A., & Newman, E. A. (2010). Glial and neuronal control of brain blood flow. *Nature*, 468(7321), 232.

Bandettini, P. A., Wong, E. C., Hinks, R. S., Tikofsky, R. S., & Hyde, J. S. (1992). Time course EPI of human brain function during task activation. *Magnetic Resonance in Medicine*, 25(2), 390-397.

Barnett, A., Marty-Dugas, J., & McAndrews, M. P. (2014). Advantages of sentence-level fMRI language tasks in presurgical language mapping for temporal lobe epilepsy. *Epilepsy & Behavior, 32*, 114-120. doi:10.1016/j.yebeh.2014.01.010

Binder, J. R., Frost, J. A., Hammeke, T. A., Cox, R. W., Rao, S. M., & Prieto, T. (1997). Human brain language areas identified by functional magnetic resonance imaging. *Journal of Neuroscience*, *17*(1), 353-362.

Biswal, B., Deyoe, E. A., & Hyde, J. S. (1996). Reduction of physiological fluctuations in fMRI using digital filters. *Magnetic Resonance in Medicine*, 35(1), 107-113.

Bren, K. L., Eisenberg, R., & Gray, H. B. (2015). Discovery of the magnetic behavior of hemoglobin: A beginning of bioinorganic chemistry. *Proceedings of the National Academy of Sciences*, 112(43), 13123-13127.

Buxton, R. B. (2013). The physics of functional magnetic resonance imaging (fMRI). *Reports on Progress in Physics. Physical Society (Great Britain)*, 76(9), 096601. http://doi.org/10.1088/0034-4885/76/9/096601

Chao-Gan, Y., & Yu-Feng, Z. (2010). DPARSF: a MATLAB toolbox for "pipeline" data analysis of resting-state fMRI. *Frontiers in systems neuroscience*, 4.

Cox, R. W. (1996). AFNI: software for analysis and visualization of functional magnetic resonance neuroimages. *Computers and Biomedical Research*, 29(3), 162-173.

De Araujo, D. B., Tedeschi, W., Santos, A. C., Elias, J., Neves, U. P. C., & Baffa, O. (2003). Shannon entropy applied to the analysis of event-related fMRI time series. *NeuroImage*, 20(1), 311–317. http://doi.org/10.1016/S1053-8119(03)00306-9

DeCharms, R. C., Christoff, K., Glover, G. H., Pauly, J. M., Whitfield, S., & Gabrieli, J. D. E. (2004). Learned regulation of spatially localized brain activation using real-time fMRI. *NeuroImage*, 21(1), 436–443. http://doi.org/10.1016/j.neuroimage.2003.08.041

Desmond, J. E., & Chen, S. A. (2002). Ethical issues in the clinical application of fMRI: factors affecting the validity and interpretation of activations. *Brain and cognition,* 50(3), 482-497.

Forman, S. D., Cohen, J. D., Fitzgerald, M., Eddy, W. F., Mintun, M. A., & Noll, D. C. (1995). Improved assessment of significant activation in functional magnetic resonance imaging (fMRI): use of a cluster-size threshold. *Magnetic Resonance in Medicine,* 33(5), 636-647.

Friston, K. J., Holmes, A. P., Worsley, K. J., Poline, J. P., Frith, C. D., & Frackowiak, R. S. (1994). Statistical parametric maps in functional imaging: a general linear approach. *Human brain mapping*, 2(4), 189-210.

Friston, K. J., Mechelli, A., Turner, R., & Price, C. J. (2000). Nonlinear responses in fMRI: the Balloon model, Volterra kernels, and other hemodynamics. *NeuroImage*, 12(4), 466-477.

FSL Course (2016). Retrieved June 21, 2017, from FMRIB Analysis Group & MGH Lecture Slides & Practical Data (2016 Course) website, https://fsl.fmrib.ox.ac.uk/fslcourse/lectures/feat1_part1.pdf

Gaillard, W. D., Balsamo, L., Xu, B., McKinney, C., Papero, P. H., Weinstein, S., ... & Vezina, L. G. (2004). fMRI language task panel improves determination of language dominance. *Neurology*, 63(8), 1403-1408.

Greve, D. N., Brown, G. G., Mueller, B. A., Glover, G., & Liu, T. T. (2013). A survey of the sources of noise in fMRI. *Psychometrika*, 78(3), 396-416.

Hamberger M.J. & Cole J. (2011). Language organization and reorganization in epilepsy. *Neuropsychology Reviews*, 21, 240.

Handwerker, D. A., Ollinger, J. M., & D'Esposito, M. (2004). Variation of BOLD hemodynamic responses across subjects and brain regions and their effects on statistical analyses. *NeuroImage*, 21(4), 1639-1651.

Henson, R. N. A., & Rugg, M. D. (2003). Neural response suppression, haemodynamic repetition effects, and behavioural priming. *Neuropsychologia*, 41(3), 263-270.

Iadecola, C., & Nedergaard, M. (2007). Glial regulation of the cerebral microvasculature. *Nature Neuroscience*, 10(11), 1369.

Isaaks K.L., Barr W.B., Nelson P.K., & Devisky O. (2006). Degree of handedness and cerebral dominance. *Neurology*, 66(12), 1855.2

Janecek, J. K., Swanson, S. J., Sabsevitz, D. S., Hammeke, T. A., Raghavan, M., E. Rozman, M., & Binder, J. R. (2013). Language lateralization by fMRI and Wada testing in 229 patients with epilepsy: Rates and predictors of discordance. *Epilepsia*, 54(2), 314–322. http://doi.org/10.1111/epi.12068

Jansen, A., Menke, R., Sommer, J., Förster, A. F., Bruchmann, S., Hempleman, J., … Knecht, S. (2006). The assessment of hemispheric lateralization in functional MRI-Robustness and reproducibility. *NeuroImage*, 33(1), 204–217. http://doi.org/10.1016/j.neuroimage.2006.06.019

Jenkinson, M., Beckmann, C. F., Behrens, T. E., Woolrich, M. W., & Smith, S. M. (2012). Fsl. *Neuroimage*, 62(2), 782-790.

Jones-Gotman, M., Sziklas, V., & Djordjevic, J. (2009). Intracarotid amobarbital procedure and etomidate speech and memory test. *Canadian Journal of Neurological Sciences*, 36.

Karahanoğlu, F. I., Caballero-Gaudes, C., Lazeyras, F., & Van De Ville, D. (2013). Total activation: fMRI deconvolution through spatio-temporal regularization. *NeuroImage*, 73, 121-134.

Kochiyama, T., Morita, T., Okada, T., Yonekura, Y., Matsumura, M., & Sadato, N. (2005). Removing the effects of task-related motion using independent-component analysis. *NeuroImage*, 25(3), 802-814.

Liddle, P. F., Kiehl, K. A., & Smith, A. M. (2001). Event-related fMRI study of response inhibition. *Human brain mapping*, 12(2), 100-109.

Mazziotta, J. C., Toga, A. W., Evans, A., Fox, P., & Lancaster, J. (1995). A probabilistic atlas of the human brain: Theory and rationale for its development: The international consortium for brain mapping (icbm). *NeuroImage*, 2(2), 89-101.

Morrison, C. (2010). *Handbook on the Neuropsychology of Epilepsy*. W. B. Barr (Ed.). Springer.

Müller, R. A., Rothermel, R. D., Behen, M. E., Muzik, O., Mangner, T. J., & Chugani, H. T. (1997). Receptive and expressive language activations for sentences: a PET study. *Neuroreport*, *8*(17), 3767-3770.

Neele, S. J., Rombouts, S. A., Bierlaagh, M. A., Barkhof, F., Scheltens, P., & Netelenbos, J. C. (2001). Raloxifene affects brain activation patterns in postmenopausal women during visual encoding. *The Journal of Clinical Endocrinology & Metabolism*, *86*(3), 1422-1422.

Negishi, M., Martuzzi, R., Novotny, E. J., Spencer, D. D., & Constable, R. T. (2011). Functional MRI connectivity as a predictor of the surgical outcome of epilepsy. *Epilepsia*, 52(9), 1733–1740. http://doi.org/10.1111/j.1528-1167.2011.03191.x

Ogawa, S., Lee, T. M., Kay, A. R., & Tank, D. W. (1990). Brain magnetic resonance imaging with contrast dependent on blood oxygenation. *Proceedings of the National Academy of Sciences*, 87(24), 9868-9872.

Ogawa, S., Lee, T. M., Nayak, A. S., & Glynn, P. (1990). Oxygenation-sensitive contrast in magnetic resonance image of rodent brain at high magnetic fields. *Magnetic Resonance in Medicine*, 14(1), 68-78.

O'Grady, C., Omisade, A., & Sadler, R. M. (2016). Language lateralization of a bilingual person with epilepsy using a combination of fMRI and neuropsychological assessment findings. *Neurocase*, *22*(5), 1–7. http://doi.org/10.1080/13554794.2016.1233987

Ostwald, D., & Bagshaw, A. P. (2011). Information theoretic approaches to functional neuroimaging, *Magnetic Resonance Imaging,* 29, 1417–1428. http://doi.org/10.1016/j.mri.2011.07.013

Ostwald, D., Porcaro, C., & Bagshaw, A. P. (2011). Voxel-wise information theoretic EEG-fMRI feature integration. *NeuroImage*, 55(3), 1270-1286.

Patel, A. X., Kundu, P., Rubinov, M., Jones, P. S., Vértes, P. E., Ersche, K. D., ... & Bullmore, E. T. (2014). A wavelet method for modeling and despiking motion artifacts from resting-state fMRI time series. *NeuroImage*, 95, 287-304.

Pincus, S. M., Gladstone, I. M., & Ehrenkranz, R. A. (1991). A regularity statistic for medical data analysis. *Journal of Clinical Monitoring and Computing*, 7(4), 335-345.

Power, J. D., Schlaggar, B. L., & Petersen, S. E. (2015). Recent progress and outstanding issues in motion correction in resting state fMRI. *NeuroImage*, 105, 536-551.

Pruim, R. H., Mennes, M., Buitelaar, J. K., & Beckmann, C. F. (2015). Evaluation of ICA-AROMA and alternative strategies for motion artifact removal in resting state fMRI. *NeuroImage*, 112, 278-287.

Satterthwaite, T. D., Elliott, M. A., Gerraty, R. T., Ruparel, K., Loughead, J., Calkins, M. E., ... & Wolf, D. H. (2013). An improved framework for confound regression and filtering for control of motion artifact in the preprocessing of resting-state functional connectivity data. *NeuroImage*, 64, 240-256.

Segaert, K., Weber, K., de Lange, F. P., Petersson, K. M., & Hagoort, P. (2013). The suppression of repetition enhancement: a review of fMRI studies. *Neuropsychologia*, 51(1), 59-66.

Siegel, J. S., Mitra, A., Laumann, T. O., Seitzman, B. A., Raichle, M., Corbetta, M., & Snyder, A. Z. (2016). Data Quality Influences Observed Links Between Functional Connectivity and Behavior. *Cerebral Cortex*, 1–11. http://doi.org/10.1093/cercor/bhw253

Smith, A. M., Lewis, B. K., Ruttimann, U. E., Frank, Q. Y., Sinnwell, T. M., Yang, Y., ... & Frank, J. A. (1999). Investigation of low frequency drift in fMRI signal. *NeuroImage*, 9(5), 526-533.

Smith, S. M. (2004). Overview of fMRI analysis. *The British Journal of Radiology*, 77(suppl_2), S167-S175.

snr Documentation. (n.d.). Retrieved March 3, 2017, from *Mathworks Documentation* website, https://www.mathworks.com/help/signal/ref/snr.html

Soon, C. S., Venkatraman, V., & Chee, M. W. (2003). Stimulus repetition and hemodynamic response refractoriness in event-related fMRI. *Human brain mapping*, 20(1), 1-12.

Steffener, J., Tabert, M., Reuben, A., & Stern, Y. (2010). Investigating hemodynamic response variability at the group level using basis functions. *Neuroimage*, *49*(3), 2113-2122.

Stippich, C. (2010). Presurgical functional magnetic resonance imaging. *Der Radiologe*, 50(2), 110-122.

Tanaka, N., & Stufflebeam, S. M. (2016). Presurgical Mapping of the Language Network Using Resting-state Functional Connectivity. *Topics in Magnetic Resonance Imaging*, 25(1), 19–23. http://doi.org/10.1097/RMR.0000000000000073

Tedescschi, W., Müller, H. P., de Araujo, D. B., Santos, A. C., Neves, U. P. C., Ernè, S. N., & Baffa, O. (2005). Generalized mutual information tests applied to fMRI analysis. *Physica A: Statistical Mechanics and its Applications*, 352(2), 629-644.

Tikhonov, A. N. (1963). "О решени и некорректно поставленных задач и методе регуляризац ии". Doklady Akademii Nauk SSSR. 151: 501–504. Translated in "Solution of incorrectly formulated problems and the regularization method". *Soviet Mathematics*. 4: 1035–1038.

Vakkuri, A., Yli-Hankala, A., Talja, P., Mustola, S., Tolvanen-Laakso, H., Sampson, T., & Viertiö-Oja, H. (2004). Time-frequency balanced spectral entropy as a measure of anesthetic drug effect in central nervous system during sevoflurane, propofol, and thiopental anesthesia. *Acta Anaesthesiologica Scandinavica*, 48(2), 145-153.

Van Essen, D. C., Smith, S. M., Barch, D. M., Behrens, T. E., Yacoub, E., Ugurbil, K., & Wu-Minn HCP Consortium. (2013). The WU-Minn human connectome project: an overview. *NeuroImage*, 80, 62-79.

Wada, J. (1949). A new method of determining the side of cerebral speech dominance: a preliminary report on the intracarotid injection of sodium amytal in man. *Igaku to seibutsugaki*, 14, 221-222.

Wang, Z., Li, Y., Childress, A. R., & Detre, J. A. (2014). Brain entropy mapping using fMRI. *PLoS ONE*, 9(3). http://doi.org/10.1371/journal.pone.0089948

Welvaert, M., Durnez, J., Moerkerke, B., Verdoolaege, G., & Rosseel, Y. (2011). neuRosim: An R package for generating fMRI data. *Journal of Statistical Software*, 44(10), 1–18. http://doi.org/10.18637/jss.v044.i10

Yakupov, R., Lei, J., Hoffmann, M., & Speck, O. (2017). False fMRI activation after motion correction. *Human Brain Mapping*.

Ying, L., Xu, D., & Liang, Z. P. (2004, September). On Tikhonov regularization for image reconstruction in parallel MRI. In *Engineering in Medicine and Biology Society, 2004. IEMBS'04. 26th Annual International Conference of the IEEE* (Vol. 1, pp. 1056-1059). IEEE.

Yousry, T. A., Schmid, U. D., Jassoy, A. G., Schmidt, D., Eisner, W. E., Reulen, H. J., ... & Lissner, J. (1995). Topography of the cortical motor hand area: prospective study with functional MR imaging and direct motor mapping at surgery. *Radiology*, 195(1), 23-29.